COMPOSITE ANALYSIS OF HEAVY SNOW EVENTS WITHIN THE SPRINGFIELD AND ST. LOUIS, MISSOURI NATIONAL WEATHER SERVICE COUNTY WARNING AREAS

Jayson P. Gosselin
Chad M. Gravelle
Charles E. Graves
Saint Louis University
Earth and Atmospheric Sciences
St. Louis, Missouri

John P. Gagan
NOAA/National Weather Service
Weather Forecast Office
Springfield, Missouri

Fred H. Glass
NOAA/National Weather Service
Weather Forecast Office
St. Louis, Missouri

Abstract

A climatology and composite analysis of 28 cold season (October 1980 – March 2008) heavy snow events within the Springfield (SGF) and St. Louis, Missouri (LSX) National Weather Service (NWS) County Warning Areas (CWAs) are presented utilizing snowfall data from the National Climatic Data Center (NCDC) Cooperative Summary of the Day (COOP) collection. COOP snow events with amounts greater than 6 in. (15.24 cm) in at least one CWA were identified as heavy snow cases. Sixty-four heavy snow cases were identified for the period of study and were then classified based on the orientation of the axis of greatest snowfall. This procedure yielded 36 southwest-northeast (SW/NE) oriented cases, 21 west-east (W/E) cases, 5 northwest-southeast (NW/SE) cases, and two "other" cases where there was no well-defined axis of greatest snowfall orientation. Since the most common orientation was SW/NE, these cases were investigated further.

System-relative composites were generated using the General Meteorological Package (GEMPAK) and the North American Regional Reanalysis (NARR) dataset, where the initial analysis time (i.e., t = 0 h) for each SW/NE case was defined as the date and time when the NARR 850-hPa low was closest to the 92nd meridian. Composites were also calculated at 6-h intervals beginning 12 h before (t = -12 h) to 12 h after (t = +12 h) the initial analysis time to depict the evolution of features associated with heavy snow-producing systems in the region. The composites indicated the presence of large-scale ascent through jet-streak interaction and differential positive vorticity advection. As the composite system entered the region, an increase in mesoscale forcing collocated within an area of large-scale ascent developed over the study area in association with strengthening low-level frontogenesis and reduced symmetric stability. In addition, a case study was presented to illustrate how the composite fields are characteristic of an individual event. Finally, case-by-case variability was investigated by comparing the individual cases with the composited fields through a statistical analysis to assist in determining the degree of representativeness of the composite fields.

Corresponding Author: Jayson P. Gosselin
Saint Louis University, Earth and Atmospheric Sciences
3642 Lindell Blvd., St. Louis, MO 63108
E-mail: gosseljp@slu.edu

1. Introduction

Annually, an average of 105 snow-producing storm systems generates hazardous weather conditions that affect the contiguous United States (Adams et al. 2004). These storms result in substantial economic damages in terms of removal costs, delays in ground and air transportation, food damage due to snowmelt, damage to crops and livestock, accidents, injuries, and loss of life (Adams et al. 2004). The subsequent societal and economic impacts make it imperative to work toward improving both the quality and lead time of winter weather forecasts. Increasing forecasters' experience, particularly when that experience can be acquired in the same area over many years, can improve forecast accuracy (Schmit and Hultquist 2009). A key benefit of such experience is increased skill in pattern recognition, which helps to better identify potentially significant weather events (Schmit and Hultquist 2009).

Early climatological studies of snowstorms focused on classifying events on a regional scale (e.g., Midwest - see Changnon 1969; Changnon and Changnon 1978). Changnon (1969), in a climatological study of severe winter storms in Illinois, found that the most frequent orientation of heavy snow cores [≥ 6 in. (15.24 cm)] was in a 40-degree sector from 226 through 265 degrees (i.e., oriented southwest-northeast). The study also showed that the most frequent surface low pressure track began near Colorado or the western Great Plains and moved into the junction of the Mississippi-Ohio River basins and continued northeastward into Lower Michigan. These results suggested that a southwest-northeast track is common for heavy snow events in this region.

Previous composite studies (e.g., Brandes and Spar 1971; Mote et al. 1997; Novak et al. 2004, 2010, and references therein) have shown the effectiveness of using a composite analysis approach to diagnose the synoptic and mesoscale phenomena associated with heavy snow events. However, a majority of heavy snow compositing studies have generally neglected the midwestern United States. Notable exceptions are Fawcett and Saylor (1965), Goree and Younkin (1966) and Browne and Younkin (1970).

This study uses the National Climatic Data Center (NCDC) Cooperative Summary of the Day (COOP) collection during 28 cold seasons (October 1980 - March 2008) to establish a heavy snow [≥ 6 in. (15.24 cm)] climatology for the Springfield (SGF) and St. Louis, Missouri (LSX) National Weather Service (NWS) County Warning Areas (CWAs). The climatology led to the development of the system-relative composites presented in this paper to illustrate the synoptic-scale and mesoscale evolution of features associated with heavy snow-producing systems. These subregional composites provide enhanced situational awareness and impact potential for forecasters not only within the aforementioned CWAs, but also to areas downstream because of the observation that heavy snow continued to the northeast as the composite system progressed. The paper is organized in the following manner: Section 2 describes the datasets utilized and the methodologies employed to create the heavy snow climatology and resulting composite analysis. Section 3 examines the composite fields and their evolutions. In section 4, a case study illustrates how the composites presented are representative of an individual event. Case-by-case variability is investigated in section 5, and concluding remarks are given in section 6.

2. Data and Methodology

a. Data sources

Snowfall data were obtained from the NCDC COOP collection. These data represent daily observations taken by trained weather observers. While Doesken and Judson (1996) stated that discrepancies of snowfall measurements occur due to both the conditions under which they are made, and the number of observations made, a study of Illinois storms [≥ 6 in. (15.24 cm)] by Changnon (1969) revealed that there were consistent patterns of snowfall among adjacent stations. Thus, even though there is measurement problems associated with snowfall data, it is consistent enough to pursue long-term climatological analyses, such as in Baxter et al. (2005) and Changnon et al. (2006).

The North American Regional Reanalysis (NARR) dataset grids were obtained from the National Center for Atmospheric Research. The NARR dataset uses a combination of the National Centers for Environmental Prediction (NCEP) Eta model and the Regional Data Assimilation System (RDAS), which is run over North America to act as a subset of the NCEP Global Reanalysis (Mesinger et al. 2006). The dataset has a 3-h temporal resolution with a 32-km horizontal grid spacing on 29 pressure levels. The vertical spacing is 25 hPa from 1000 hPa to 700 hPa and 275 hPa to 100 hPa, while the spacing is 50 hPa between 650 hPa and 300 hPa.

b. Methodology

First, an organized snow event database was created for the 28 cold seasons included in the NARR dataset, identifying all snow events which affected each CWA. This was accomplished by creating 24-h COOP snowfall analysis maps using the General Meteorological Package (GEMPAK; desJardins et al. 1991) for each day in the climatological

period. Next, snowfall event maps were created using the 24-h daily snowfall maps in conjunction with NARR surface, 850-hPa, 500-hPa, and 300-hPa height and wind fields. The NARR fields were used to assist in finding temporal and spatial continuity between consecutive days in order to categorize them as an event. Then, the COOP snowfall data for each station were objectively analyzed using a Barnes (1973) objective analysis scheme run on GEMPAK. The goal of the objective analysis was to produce physically meaningful output that had the same spatial features as a subjective analysis. The irregularly spaced data were placed to a 271 x 271 grid with approximately 10-km grid spacing. Parameters were chosen so that stations within a 35-km radius had the most influence on each grid point. Finally, a nine-point smoother was also applied to the final COOP snowfall analysis field before graphics were generated using GEMPAK (Fig. 1).

COOP snow events which exhibited amounts greater than 6 in. (15.24 cm) in at least one CWA were deemed a potential case. This procedure yielded a potential of 64 cases through the period. The cases were then categorized by the orientation of the axis of greatest snowfall. This resulted in 36 southwest-northeast (SW/NE) oriented cases, 21 west-east (W/E) cases, 5 northwest-southeast (NW/SE) cases, and two "other" cases where there was no discernible axis orientation. Since the SW/NE oriented cases comprised a majority of the total cases (36 of 64), only those cases were investigated in this particular study. All of the 36 cases included are given in Table 1.

System-relative composite analyses were created for the 36 SW/NE cases utilizing GEMPAK and the NARR dataset. The initial analysis time (t = 0 h) for each heavy snow case was defined as the time (3-h temporal resolution) and date when the NARR 850-hPa height low was closest to the 92nd meridian (Fig. 2). The 850-hPa low was tracked in this study because it has been shown to be more consistent than other fields (e.g., mean sea-level pressure) with respect to the axis of heavy snow (Goree and Younkin 1966). The 92nd meridian was chosen because it nearly bisects the region of interest. In addition, composites were calculated at 6-h intervals from 12 h before (t = -12 h) to 12 h after (t = +12 h) the initial analysis time. A 207 x 159 grid with 32-km grid spacing was then extracted from the NARR dataset centered on the 36 SW/NE 850-hPa height lows at each composite time. Parameters were averaged using a locally-written compositing program and results were then displayed using GEMPAK. The composite fields were examined and a subset of the results is presented in the following section.

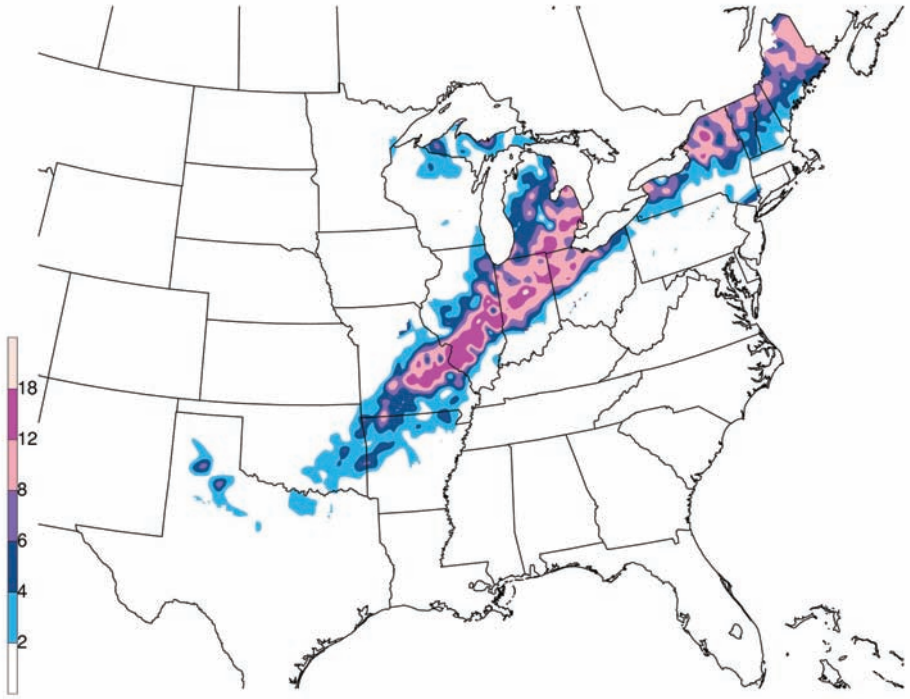

Fig. 1. Example of a SW/NE oriented heavy snow case depicting snowfall accumulation [inches] for the 72-h period ending at 1200 UTC 01 February 1982 based upon COOP station data from NCDC.

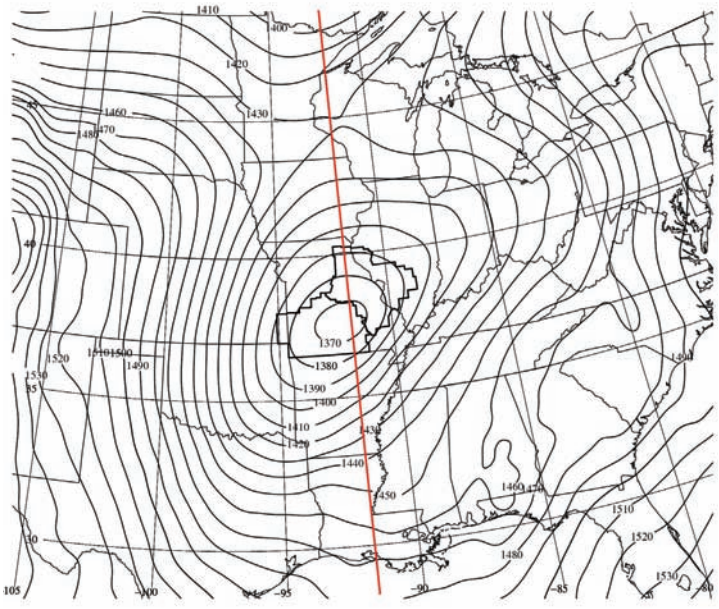

Fig. 2. Example of determining the initial analysis time (t = 0 h) using NARR 850-hPa geopotential height [m] from 2100 UTC 15 December 2007. Red line indicates the 92nd meridian.

Storm Dates	Hour
26-28 Nov 1980	1800 UTC 26 Nov
10-11 Feb 1981	1500 UTC 10 Feb
22-23 Dec 1981	1800 UTC 22 Dec
31 Jan-01 Feb 1982	0600 UTC 31 Jan
03-04 Feb 1982	0600 UTC 03 Feb
26-28 Feb 1984	0600 UTC 27 Feb
05-06 Dec 1984	1800 UTC 05 Dec
03-04 Jan 1985	0300 UTC 01 Jan
09-10 Jan 1987	1800 UTC 09 Jan
17-19 Jan 1987	0600 UTC 19 Jan
14-15 Dec 1987	0300 UTC 15 Dec
03-04 Mar 1988	0000 UTC 04 Mar
20-21 Nov 1988	0600 UTC 20 Nov
05-07 Mar 1989	0000 UTC 06 Mar
09-10 Jan 1993	0600 UTC 10 Jan
15-16 Feb 1993	0300 UTC 16 Feb
08-09 Mar 1994	0600 UTC 09 Mar
19-20 Jan 1995	0300 UTC 19 Jan
19-20 Dec 1995	0600 UTC 19 Dec
02-03 Jan 1996	0600 UTC 02 Jan
09-10 Jan 1997	0300 UTC 09 Jan
13-15 Mar 1999	1800 UTC 13 Mar
11-12 Mar 2000	0600 UTC 11 Mar
13-14 Dec 2000	2100 UTC 13 Dec
02-03 Mar 2002	1200 UTC 02 Mar
24-25 Dec 2002	0900 UTC 24 Dec
02-03 Jan 2003	0900 UTC 02 Jan
23-24 Feb 2003	0900 UTC 22 Feb
13-14 Dec 2003	0000 UTC 14 Dec
24-25 Nov 2004	1500 UTC 24 Nov
22-23 Dec 2004	1800 UTC 22 Dec
30 Nov-01 Dec 2006	0000 UTC 01 Dec
21 Jan 2007	1800 UTC 21 Jan
15-16 Dec 2007	1800 UTC 15 Dec
31 Jan-01 Feb 2008	0000 UTC 01 Feb
04-05 Mar 2008	0300 UTC 04 Mar

Table 1. Dates of SW/NE heavy snow events included in the study and the initial analysis (t = 0 h) time for each respective event.

3. Composite Results

a. Synoptic-scale composite evolution

At the start of the compositing period (t = -12 h), a weak surface cyclone is located over eastern Texas (Fig. 3, top-left panel) associated with a positively tilted 500-hPa trough on the lee side of the Rocky Mountains (Fig. 3, bottom-left panel). At 850 hPa, there is a broad, closed circulation (Fig. 3, top-right panel) located along the Red River between Texas and Oklahoma with a southerly 30-kt low-level jet, implying the transport of warm, moist air northward from the Gulf of Mexico. Two jet streaks are present at 300 hPa: the upstream jet streak is found rounding the base of the trough while the downstream jet streak is found in an area of confluence near the eastern Great Lakes (Fig. 3, bottom-right panel). This pattern resembles the common jet configuration cited by Kocin and Uccellini (2004) for northeastern United States heavy snowstorms and suggests jet-streak interaction between the left-exit region of the upstream jet streak and the right-entrance region of the downstream jet streak (Fig. 3, bottom-right panel).

Six hours later at t = -6 h, the composite surface cyclone (Fig. 4, top-left panel) has moved slightly north of due east to the Texas-Louisiana border while maintaining its intensity from the previous composite time period. The 850-hPa low has deepened approximately 30 m in the past 6 h and moved northeastward into far southeastern Oklahoma (Fig. 4, top-right panel). These height falls are in response to the 500-hPa trough amplifying and transitioning from a positive tilt to a more neutral tilt (Fig. 4, bottom-left panel). Further upper-level support for vertical motion across southern Missouri and Illinois is noted at 300 hPa, as the area lies in a favorable position between the two aforementioned jet streaks, where increasing upper-level divergence and associated large-scale ascent is implied due to the jet-streak interaction (Fig. 4, bottom-right panel).

At the initial analysis time, the composite surface cyclone has moved to the northeast and is now located near Memphis, Tennessee (Fig. 5, top-left panel). This location puts the SGF and LSX CWAs to the north-northwest of the surface low pressure center, a location favorable for heavy snowfall. The 850-hPa closed low has deepened another 30 m as it moved northeastward to the Missouri-Arkansas border with a more pronounced low-level jet (Fig. 5, top-right panel). The slightly negative tilt of the 500-hPa shortwave trough (Fig.5, bottom-left panel), an increase in vorticity advection (implying strengthening differential positive vorticity advection), and 300-hPa flow pattern (Fig. 5, bottom-right panel) suggest that large-scale rising

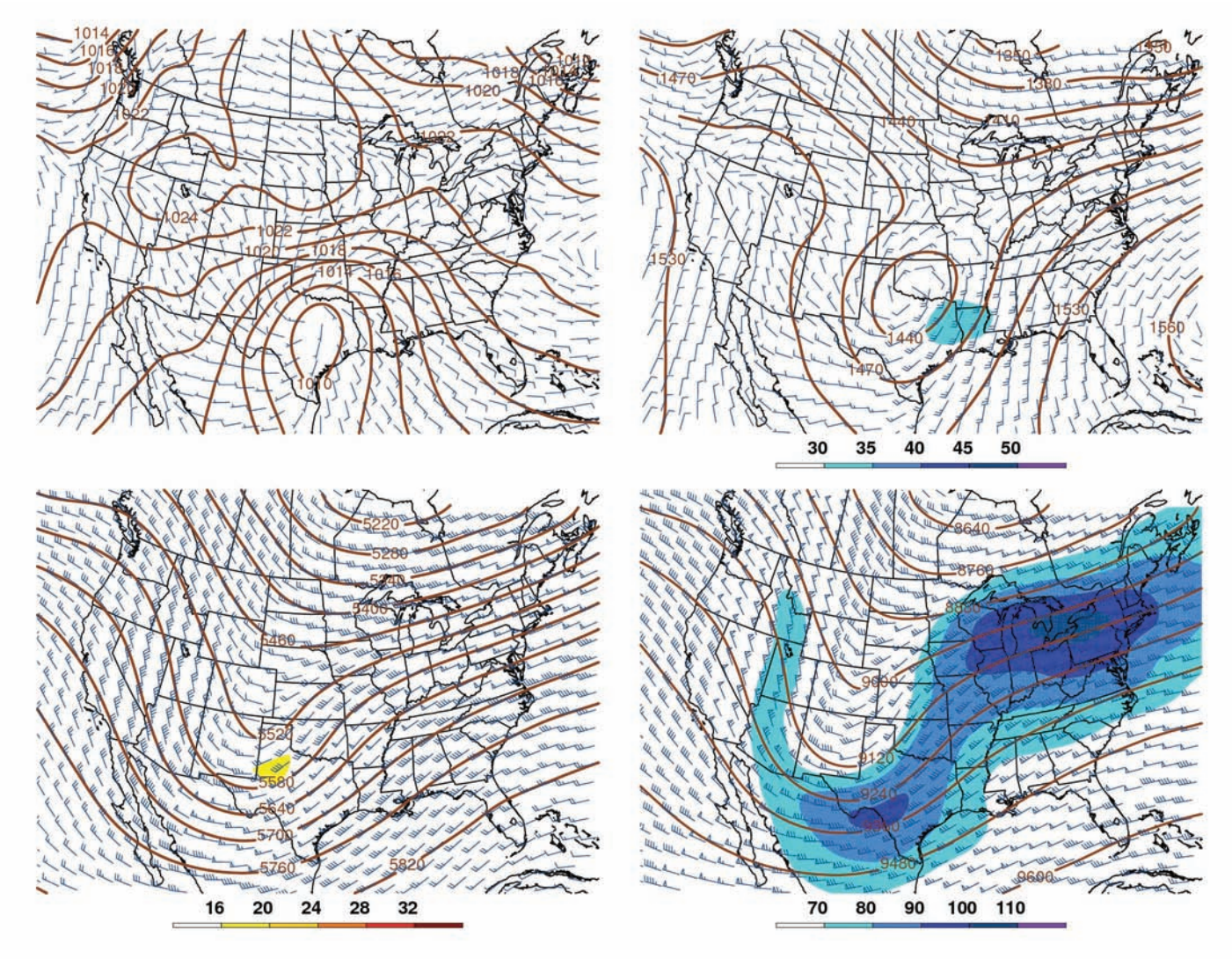

Fig. 3. Composite at t = -12 h: (top left) mean sea-level pressure [solid brown, hPa] and 10 m wind [barbs, kts]; (top right) 850-hPa geopotential height [solid brown, m], isotachs [shaded, kts], and wind [barbs, kts]; (bottom left) 500-hPa geopotential height [solid brown, m], wind [barbs, kts], and absolute vorticity [shaded,10^{-5} s^{-1}] ; (bottom right) 300-hPa geopotential height [solid brown, m], isotachs [shaded, kts], and wind [barbs, kts].

motion is present across Missouri and the mid-Mississippi Valley.

During the next 6 h, the overall composite system has continued to deepen. The surface cyclone (Fig. 6, top-left panel) has strengthened approximately 2 hPa as it tracked to the northeast with its location over western Tennessee and Kentucky. The 850-hPa low (Fig. 6, top-right panel) continues to intensify and is now centered to the southeast of St. Louis. The implied divergence associated with the coupled jet structure (Fig. 6, bottom-right panel) continues to enhance large-scale ascent over eastern Missouri and western Illinois. Of special note at this time frame is that the progression of the composite system has slowed as the 500-hPa trough has amplified and become further negatively tilted (Fig. 6, bottom-left panel), suggesting an extended duration of snowfall in the region of interest.

The composite surface cyclone (Fig. 7, top-left panel) 12 h after the initial analysis time (t = +12 h), now centered near Covington, Kentucky, continues to deepen and move to the northeast while the 850-hPa low has moved into central Indiana (Fig. 7, top-right panel). The 500-hPa trough continues to lift to the north and east (Fig. 7, bottom-left panel) while the best synoptic-scale forcing

has transitioned into portions of the Ohio River Valley.

Further evidence of forcing for large-scale ascent can be seen by investigating Q vectors. The Q-vector form of the quasi-geostrophic omega equation was shown by Hoskins et al. (1978) to describe midlatitude cyclone development and diagnose the large-scale vertical motion field. Q vectors are proportional to the strength of the horizontal ageostrophic wind and point toward rising motion, implying that convergence of Q indicates upward vertical motion while Q-vector divergence indicates downward motion. Analysis of composite 400-700-hPa layer Q vectors showed increasing total Q-vector convergence (Fig. 8) with time (t = -12 h, top left; -6 h, top right; 0 h, bottom left; + 6 h, bottom right), implying an intensification of the large-scale ascent across southern and eastern Missouri with the magnitude approximately doubling over the compositing period. Furthermore, an examination of Q-vector components in natural coordinates (as described by Keyser et al. 1992) revealed that the Q_s component constituted a majority of the total Q-vector convergence seen in Fig. 8 due to shearing deformation. However, the Q_n component, through stretching deformation, had a larger contribution to the total convergence of Q between the analysis times of t = 0 h and t = +6 h across east-central Missouri to the northwest of the midlevel cyclone, due to an increase in deformation and associated frontogenesis.

Potential vorticity (PV) analysis has been shown by previous research (e.g., Brennan et al. 2007) to be an effective tool in understanding and diagnosing upper-tropospheric dynamics in an operational setting.

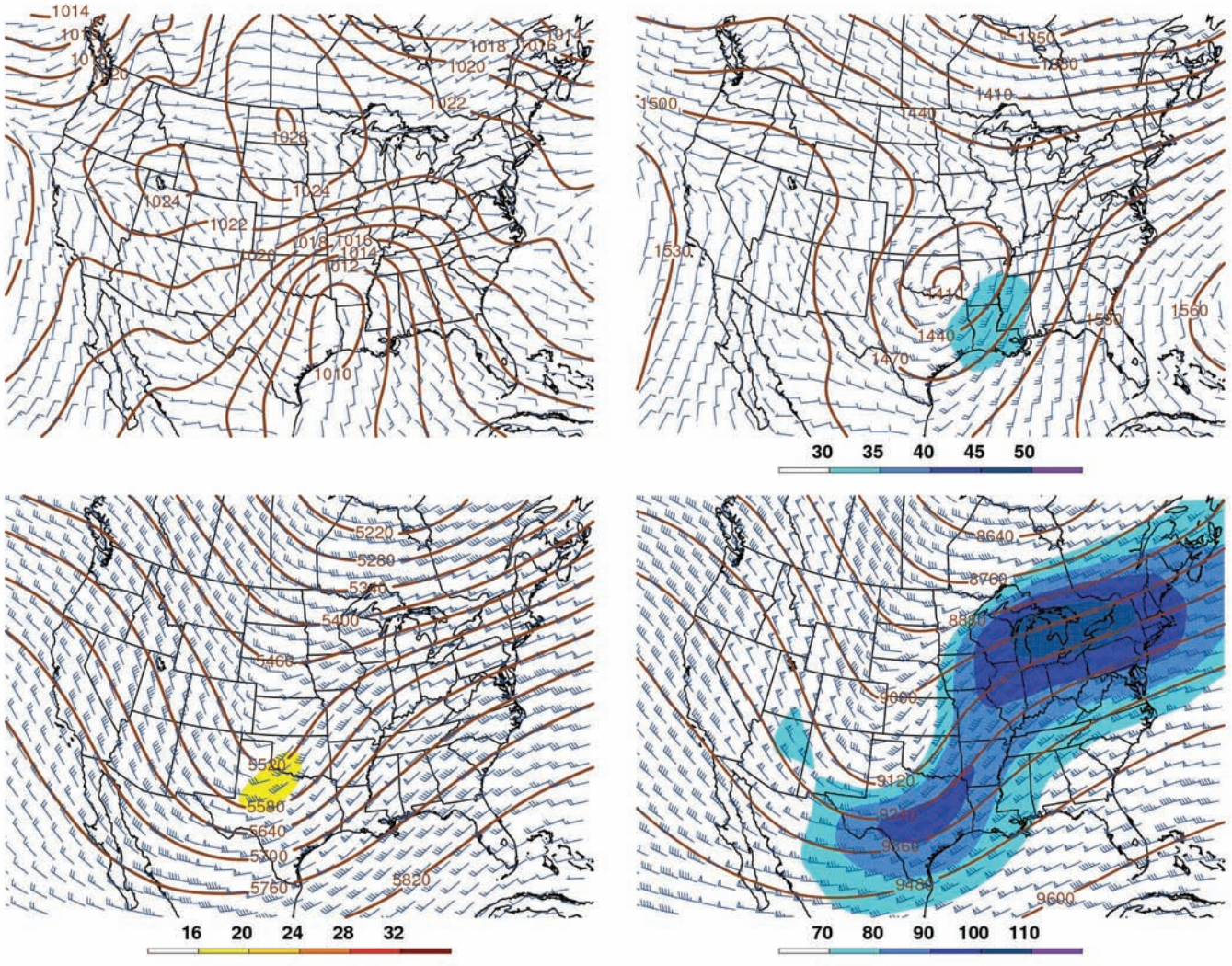

Fig. 4. As in Fig. 3, except for composite at t = - 6 h.

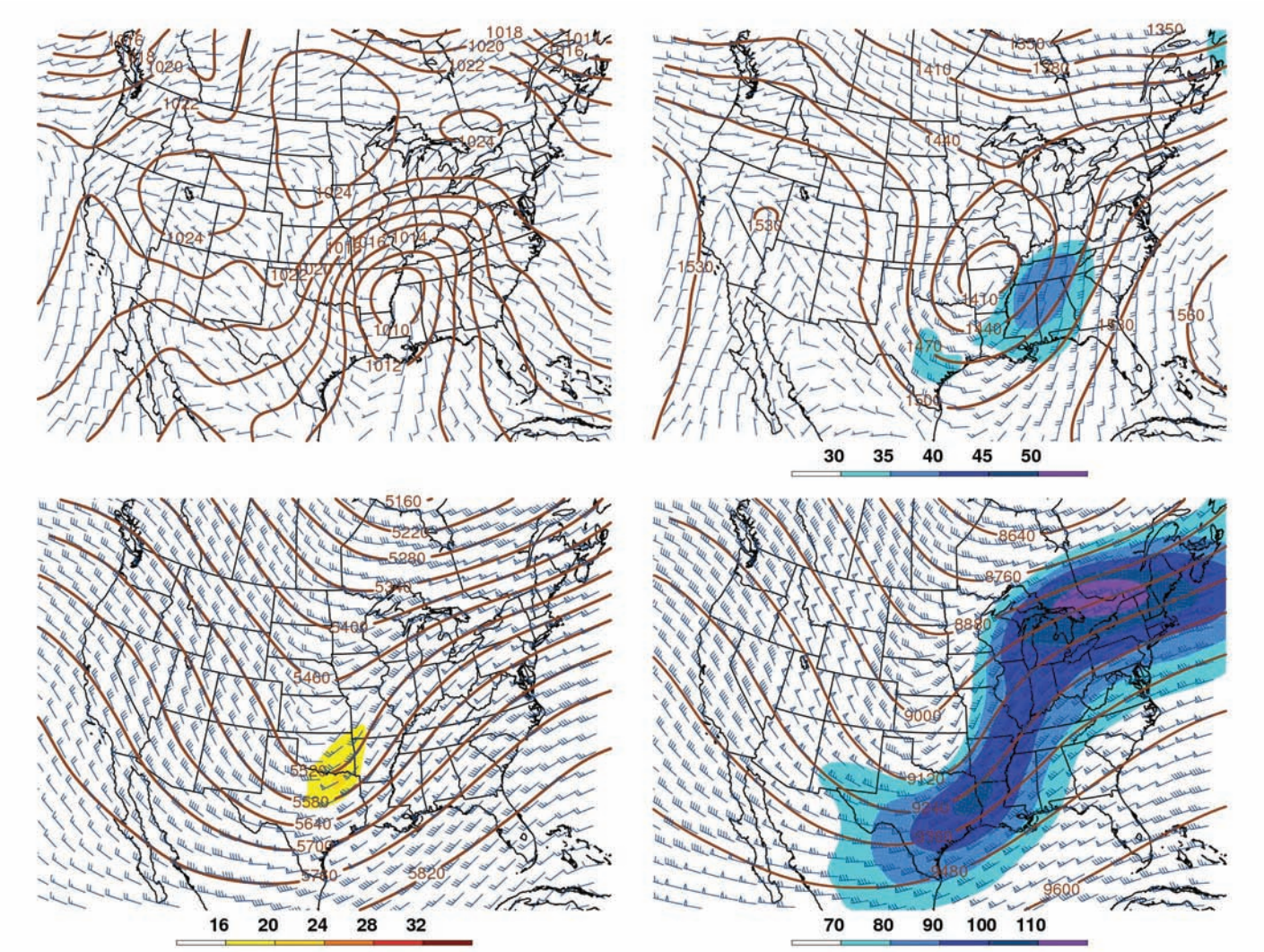

Fig. 5. As in Fig. 3, except for composite at t = 0 h.

Examination of the dynamic tropopause [typically a PV isosurface value between 1.0 and 2.0 potential vorticity units (PVU), where 1 PVU = 10^{-6} m^2 s^{-1} K kg^{-1}] can be used to diagnose PV anomalies, upper-level troughs and ridges, and jet streams. For this study, the dynamic tropopause was defined as the 1.5-PVU isosurface. Examination of this isosurface shows a cyclonic (positive) upper-tropospheric PV anomaly traveling from eastern New Mexico (Fig. 9, top-left panel) to extreme northern Arkansas (Fig. 9, bottom-right panel) from t = -12 h to t = +6 h. Strengthening of the anomaly occurs over time as indicated by rising tropopause pressures. This process is indicative of a deepening trough and an increase in associated upward vertical motion (UVM), which was exhibited in earlier composite fields. By t = +6 h, the isobar contour pattern (Fig. 9, bottom-right panel) closely resembles the treble-clef signature as shown by Martin (1998). This signature suggests that a majority of the composite members have a warm-occluded thermal structure with an associated trough of warm air aloft (TROWAL) airstream.

b. Mesoscale composite evolution

At the initial analysis time, the 850-hPa axis of frontogenesis is oriented southwest-northeast from northeast Oklahoma through southern Missouri and Illinois into southern Ohio (Fig. 10, top-left panel). The axis translates to the northeast by t = +6 h (Fig. 10, top-right panel) paralleling the track of the 850-hPa low. The 700-hPa frontogenetical axis is farther to the northwest

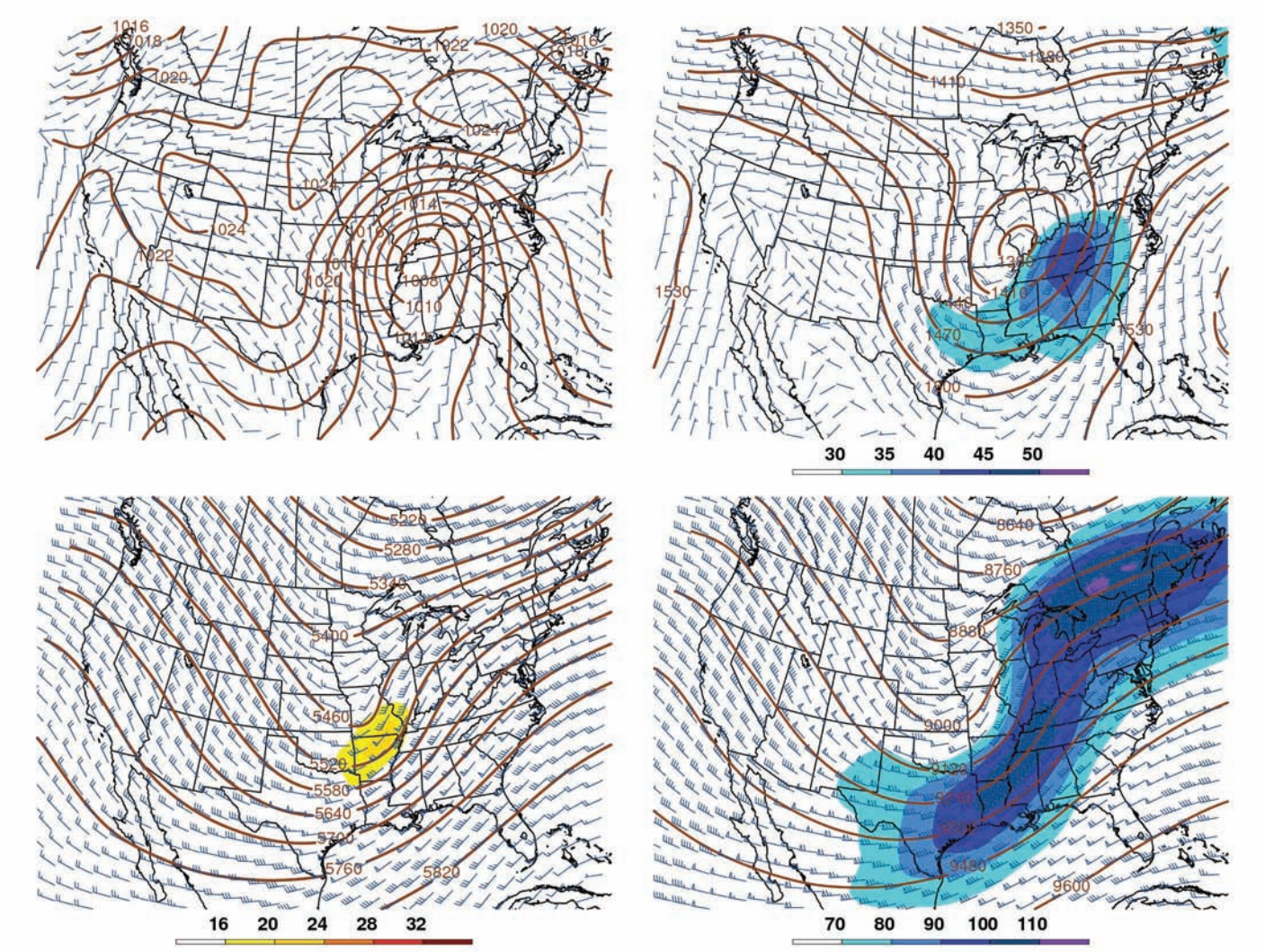

Fig. 6. As in Fig. 3, except for composite at t = +6 h.

at the initial analysis time (Fig. 10, bottom-left panel) extending from western Missouri to Lower Michigan. This axis of midlevel frontogenesis is collocated with the middle and upper-level synoptic-scale ascent, enhancing UVM in this region. The tilting of the frontogenetical axis to the northwest with height and its associated direct thermal circulation imply rising motion over central and southern regions of Missouri and Illinois. Both the 850- (Fig. 10, top-left and top-right panels) and 700-hPa frontogenetical axes (Fig. 10, bottom-left and bottom-right panels) strengthen and become better organized by t = +6 h. The midlevel frontogenesis seen in Fig. 10 is due to the contribution of warm air advection downstream of the midlevel low, and deformation to the northwest of the low associated with a developing TROWAL structure.

Composite cross-sections were taken perpendicular to the thickness gradient axis (not shown) at the initial analysis time (Fig. 11) and at t = +6 h (Fig. 12). Reduced stability is evident via greater spacing between isentropic surfaces and more vertical slopes of the 320-K (Fig. 11, top panel) and 316-K isentropes (Fig. 12, top panel) seen above the frontogenesis axis. As Emanuel (1985) noted, even small but positive moist symmetric stability can act to strengthen the intensity and decrease the scale

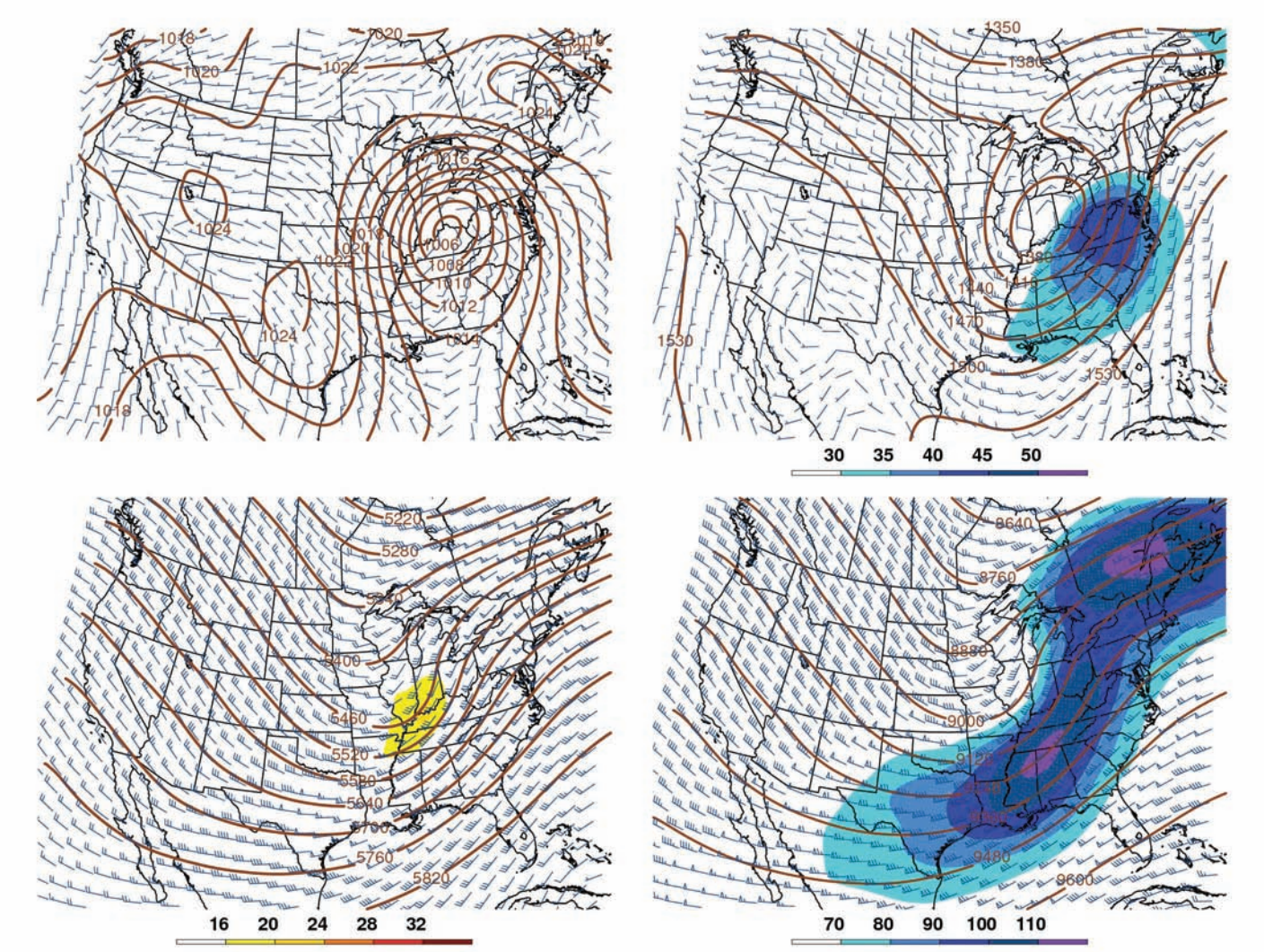

Fig. 7. As in Fig. 3, except for composite at t = +12 h.

of the UVM associated with the frontogenetical direct thermal circulation, thereby intensifying mesoscale banding. Analysis of equivalent potential vorticity (EPV) revealed weak symmetric stability in a layer above the frontogenetical axis, with a nose of weaker stability (negative EPV values) further to the south in the warm sector (Fig. 12, top panel). At the initial analysis time, the dendritic growth zone (DGZ; -12^{0}C to -18^{0}C) is nearly saturated where relative humidity values with respect to ice (RelHI) are approximately 85-95% (Fig. 11, bottom panel). In the middle of the DGZ, at -15^{0}C, there is a 80% chance of having ice nuclei in a cloud layer (Pruppacher and Klett 1997). Consequently, deposition is the process responsible for the growth of ice crystals at the expense of supercooled water droplets. Composite RelHI values at the initial analysis time show a distinctive tilting of higher saturated air toward the northwest with height (Fig. 11, bottom panel), suggesting the presence of a TROWAL associated with the cyclonic portion of the warm conveyor belt. Additionally, the vertical velocity field shows UVM occurring within the DGZ (Fig. 11, bottom panel). By t = +6 h, UVM has increased with the maximum ascent located within the DGZ (Fig. 12, bottom panel) exhibiting the cross-hair signature as shown by Waldstreicher (2001).

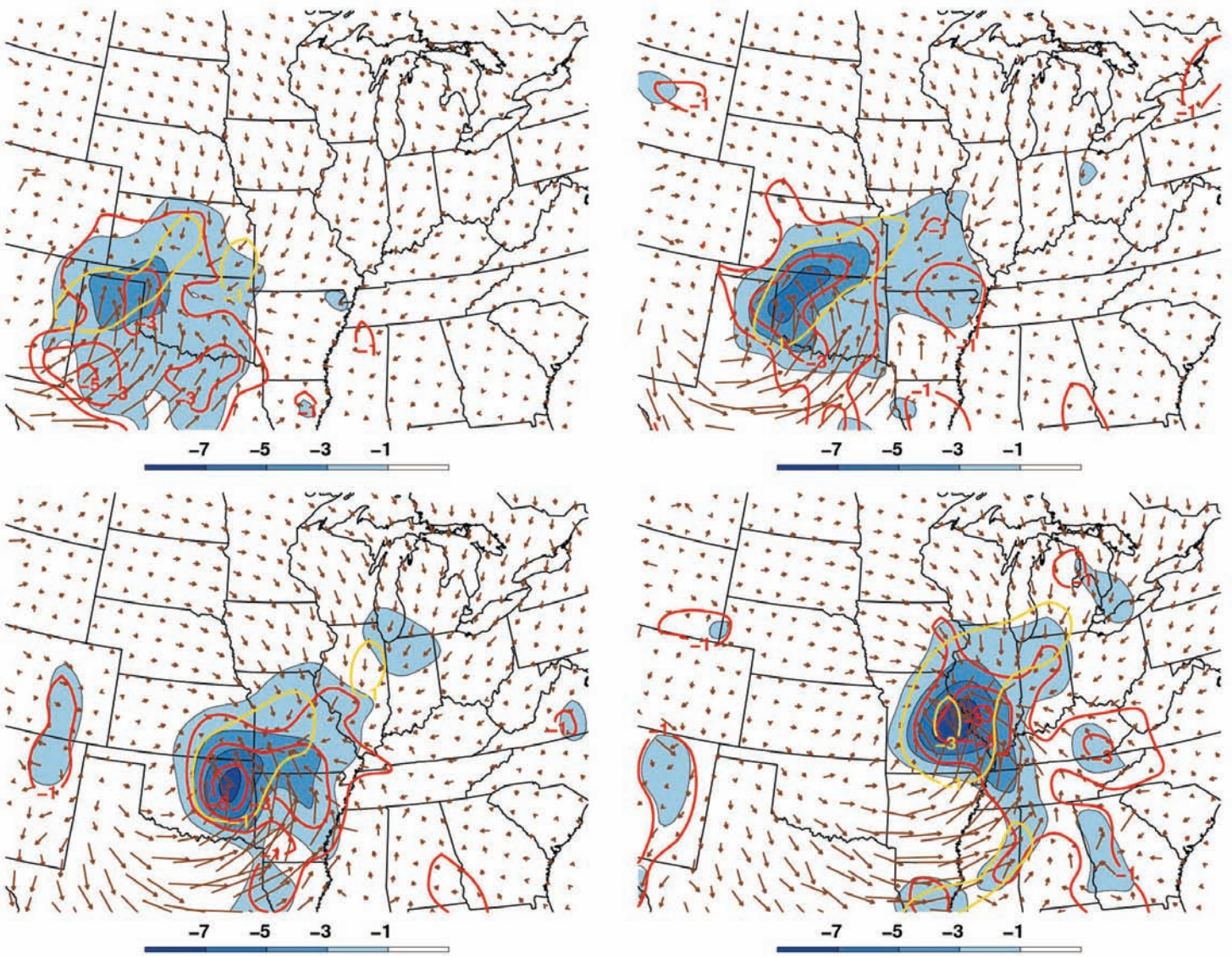

Fig. 8. Composite Q vectors in the 400-hPa to 700-hPa layer [arrows, 10^{-10} K m^{-1} s^{-1}], convergence of total Q [shaded, 10^{-14} K m^{-2} s^{-1}], convergence of Q_n [solid gold, 10^{-14} K m^{-2} s^{-1}], and convergence of Qs [solid red, 10^{-14} K m^{-2} s^{-1}]: (top left) at t = -12 h, (top right) t = -6 h, (bottom left) t = 0 h, and (bottom right) t = +6 h.

4. Case Study

To investigate the representativeness of the preceding composites, a case study is presented highlighting the synoptic and mesoscale flow evolutions as compared to the composites at key analysis times. The case selected occurred 30 January - 01 February 1982, which is a case included in the composite.

a. Overview

From 30 January to 01 February 1982, a winter storm produced a band (~175 km wide) of heavy snowfall with accumulations greater than 12 in. (30.48 cm) from east-central Missouri through Lower Michigan with isolated reports greater than 18 in. [45.72 cm; see Fig. 1]. The event began with light to moderate rain in Missouri and Illinois from 1200 UTC 30 January to 0000 UTC 31 January before rapidly changing over to snow. This band was associated with intense mesoscale forcing and reduced atmospheric stability, which produced pockets of thunder and lightning and excessive snowfall rates greater than 2 in. (5.08 cm) h^{-1}. By 1200 UTC 31 January, most of the snow had ended in the study area as the best synoptic and mesoscale forcing moved northeastward into portions of eastern Illinois and western Indiana. The impacts across the mid-Mississippi Valley were wide-ranging. Thousands of motorists were left stranded, airports and train stations closed, and many

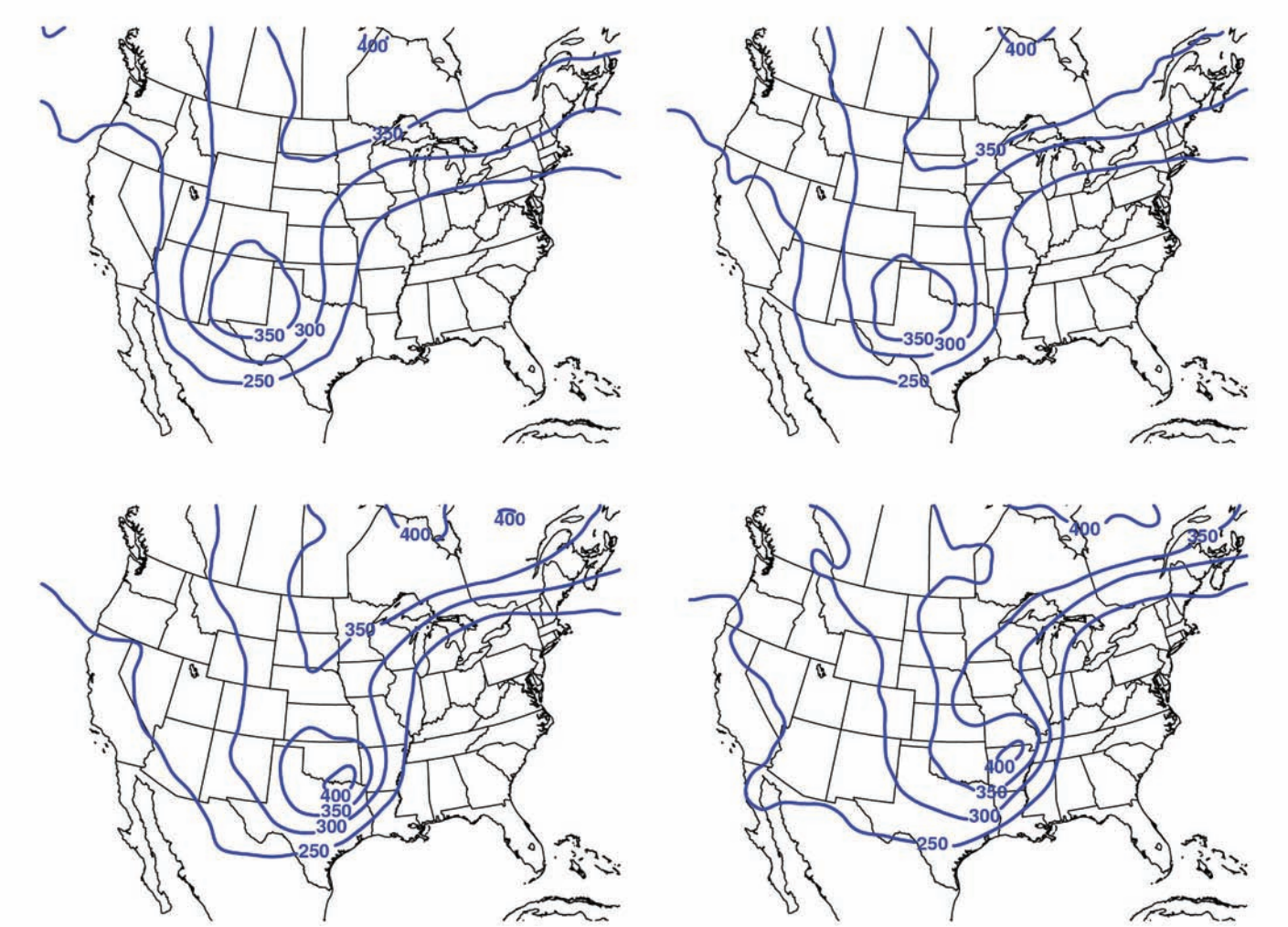

Fig. 9. Composite pressure [solid blue, hPa] on the 1.5 PVU [10^{-6} K kg^{-1} m^2 s^{-1}] surface: (top left) at t = -12 h, (top right) t = -6 h, (bottom left) t = 0 h, and (bottom right) t = +6 h.

schools and government offices were shut down for up to one full week (Moore and Blakely 1988). The city of St. Louis was one of the hardest hit areas where a snow emergency was declared, prompting the National Guard to help the city cope with the prolonged disruption to transportation.

b. Synoptic-scale evolution

Similar to the t = 0 h composite (see Fig. 5), at 0600 UTC 31 January a developing surface cyclone was located near Memphis, Tennessee (Fig. 13, top-left panel) associated with a neutrally tilted 500-hPa trough (Fig. 13, bottom-left panel). Cold northerly flow around a strong anticyclone over the eastern Dakotas (Fig. 13, top-left panel) aided in the enhancement of the low-level thermal gradient. An organized 850-hPa circulation was over northern Arkansas (Fig. 13, top-right panel) accompanied by a strong low-level jet, which helped create a well-defined deformation zone as depicted by the sudden change in wind direction from southwesterly across Tennessee and Kentucky to northeasterly from western Missouri to central Ohio. The strong deformation in the midlevel wind field helped lead to higher values of frontogenesis, which will be discussed in more detail in the following subsection. The 300-hPa flow regime revealed favorable jet-streak interaction between the left-exit region of the upstream jet streak and the right-entrance region of the downstream jet

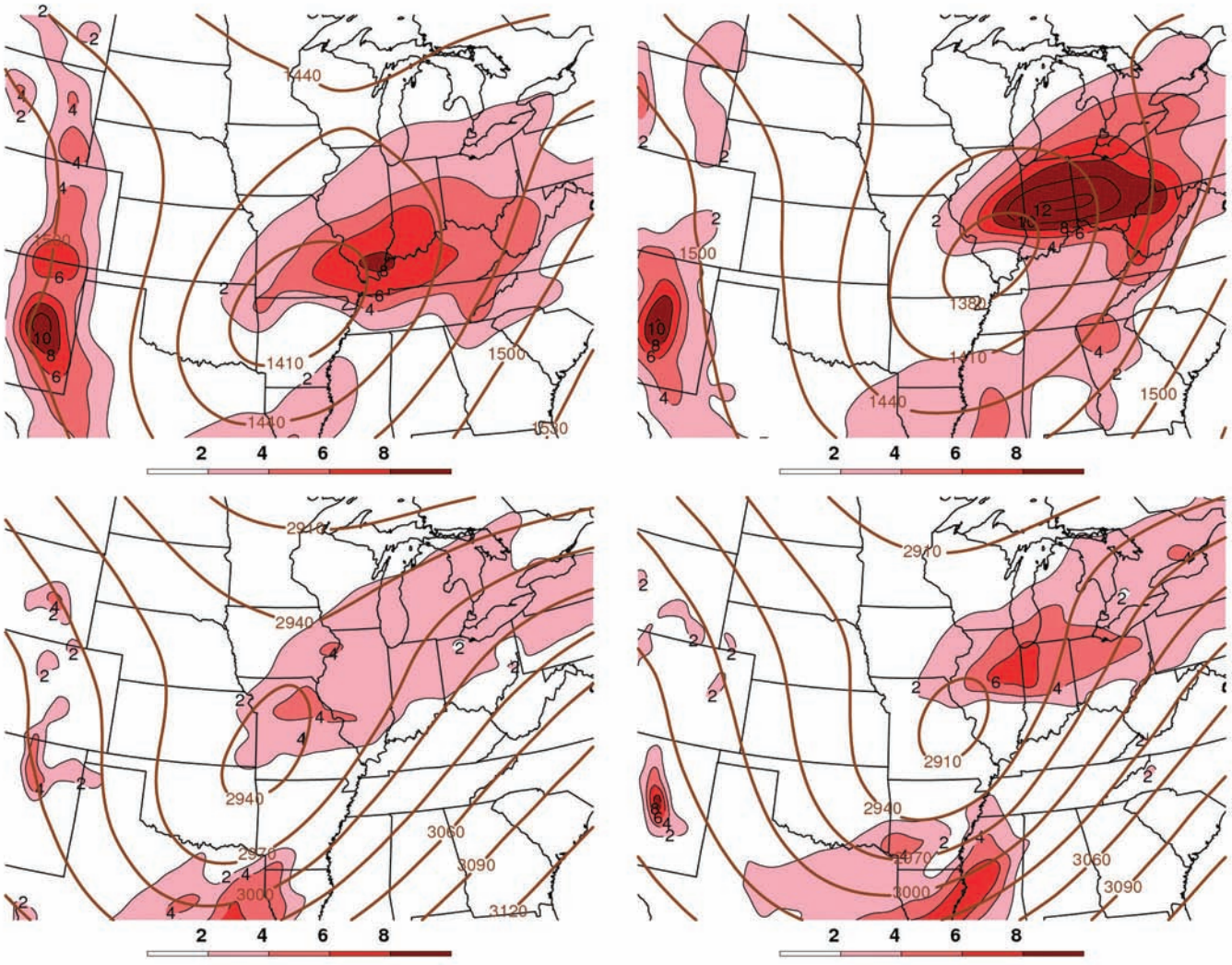

Fig, 10. Composite 850-hPa geopotential height [solid brown, m] and frontogenesis [shaded, 10^{-1} K (100 km)$^{-1}$ (3 h)$^{-1}$]: (top left) at t = 0 h and (top right) at t = +6 h; 700-hPa geopotential height [solid brown, m] and frontogenesis [shaded, 10^{-1} K (100 km)$^{-1}$ (3 h)$^{-1}$] displayed (bottom left) at t = 0 h and (bottom right) at t = +6 h.

streak (Fig. 13, bottom-right panel), implying increased upper-level divergence and associated large-scale ascent over Missouri and Illinois. This favorable jet structure was also seen in the t = 0 h composite (see Fig. 5, bottom-right panel). In addition, an upper-level confluent zone across the upper-Mississippi Valley (Fig. 13, bottom-right panel) helped to sustain and anchor the surface anticyclone to the north. Upper-level confluent flow was also seen previously in the t = 0 h composite (see Fig. 5, bottom-right panel).

By 1800 UTC 31 January, the surface cyclone continued to deepen and advanced northeastward into northern Kentucky (Fig. 14, top-left panel) while the 850-hPa low also strengthened as it proceeded into central Indiana (Fig. 14, top-right panel). The tracks of the 850-hPa and surface lows between 0600 and 1800 UTC 31 January were similar to those of the composites between the initial analysis time and t = +12 h (cf. Fig. 5 - Fig. 7, top-left and top-right panels). The 500-hPa shortwave trough at 1800 UTC has become negatively tilted (Fig. 14, bottom-

left panel), similarly to the composite 500-hPa trough at t = +12 h (see Fig. 7, bottom-left panel). Favorable jet-streak interaction at 300 hPa (Fig. 14, bottom-right panel) progressed to the northeast into the Ohio River Valley concurrent with other middle and upper-level lifting mechanisms.

Analysis of total Q-vector convergence in the 400-700-hPa layer showed a concentric maximum over the Oklahoma-Texas border at 0000 UTC 31 January (Fig. 15, top-right panel), which intensified rapidly between 0600 UTC (Fig. 15, bottom-left panel) and 1200 UTC as it advanced northeastward into extreme northern Arkansas

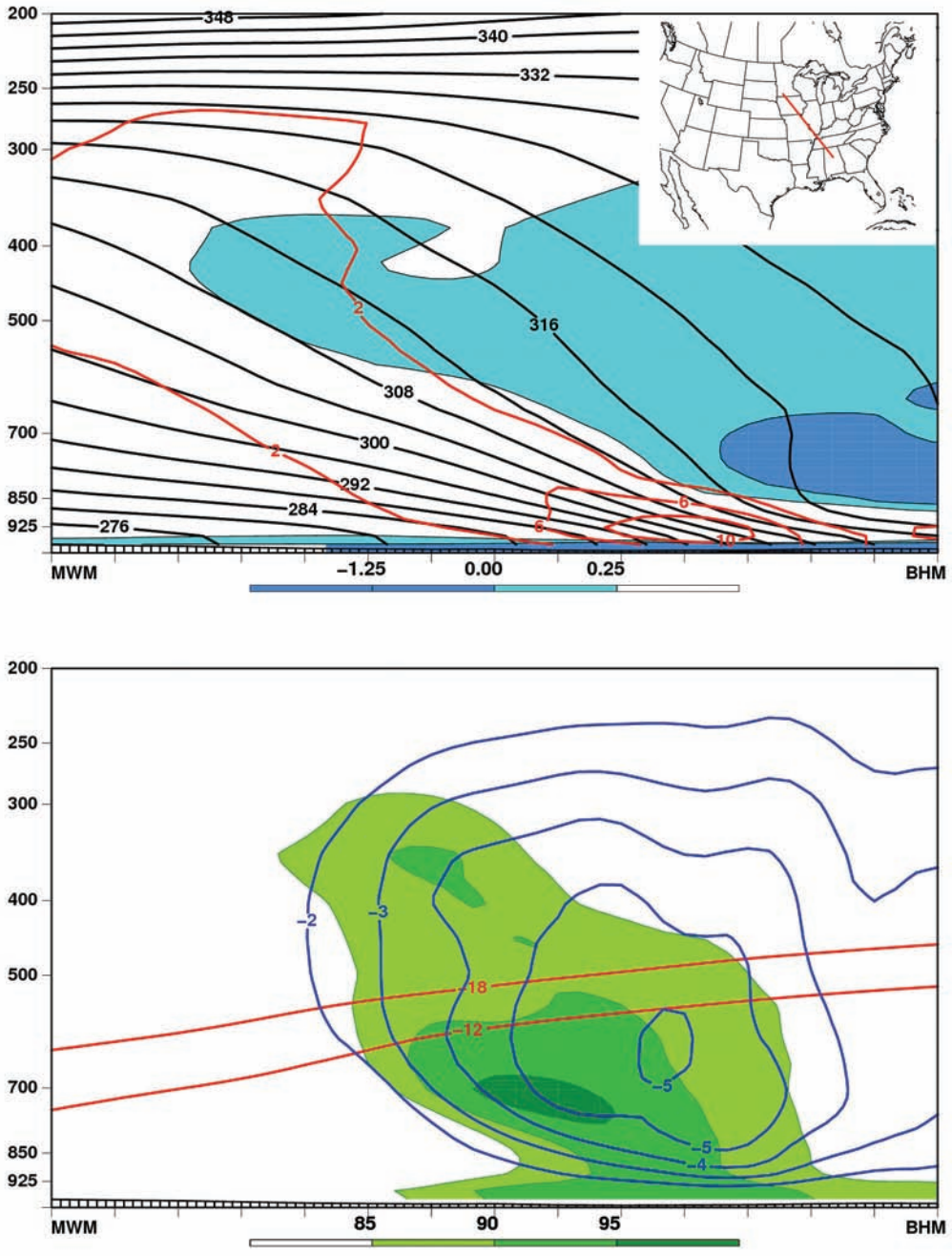

Fig. 11. (top panel) Composite cross-section showing equivalent potential vorticity [shaded, 10^{-6} K kg^{-1} m^2 s^{-1}], saturation equivalent potential temperature [solid black, K], and frontogenesis [solid red, 10^{-1} K (100 km)$^{-1}$ (3 h)$^{-1}$] at t = 0; and (bottom panel) composite cross-section showing omega [solid blue, μb s^{-1}], relative humidity with respect to ice beginning at 85% [shaded], and the dendritic growth zone from -12^{0}C to -18^{0}C [solid red, ^{0}C] at t = 0 h. Inset figure depicts the orientation of the cross-section.

(Fig. 15, bottom-right panel). The strong Q-vector convergence was collocated with an area of differential positive vorticity advection downstream of a midlevel trough. Magnitudes of total Q-vector convergence were two to three times the composite analysis values (see Fig. 8), indicating stronger forcing for large-scale ascent in the case study.

Isobars on the 1.5-PVU isosurface displayed a cyclonic PV anomaly over western Texas at 1800 UTC 30 January (Fig. 16, top-left panel). The anomaly moved to the northeast and strengthened with time, which was evident by the sharp rise in pressure of the dynamic tropopause. The strengthening of the cyclonic PV anomaly indicated a deepening upper-level trough and associated increase in large-scale ascent. A well-defined treble-clef signature was denoted at 1200 UTC 31 January (Fig. 16, bottom-right panel) with an axis of lower pressures to the northwest of the isobaric maximum. This axis or notch as shown by Posselt and Martin (2004) is caused by a diabatic erosion of PV via latent heat release, and is a feature characteristically found in the latter stages of a cyclone's life cycle.

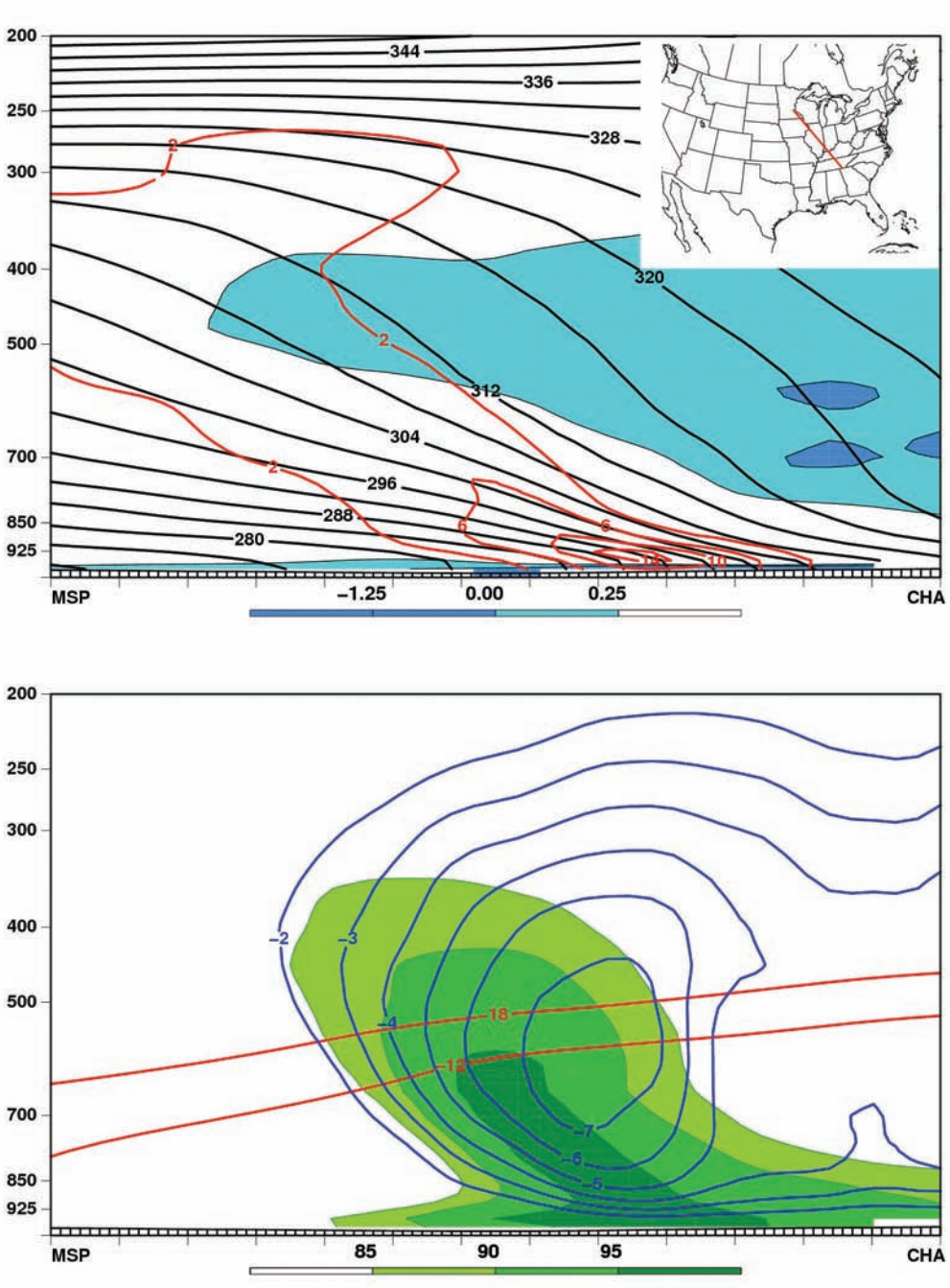

Fig. 12. As in Fig. 11, except for composite at t = +6 h.

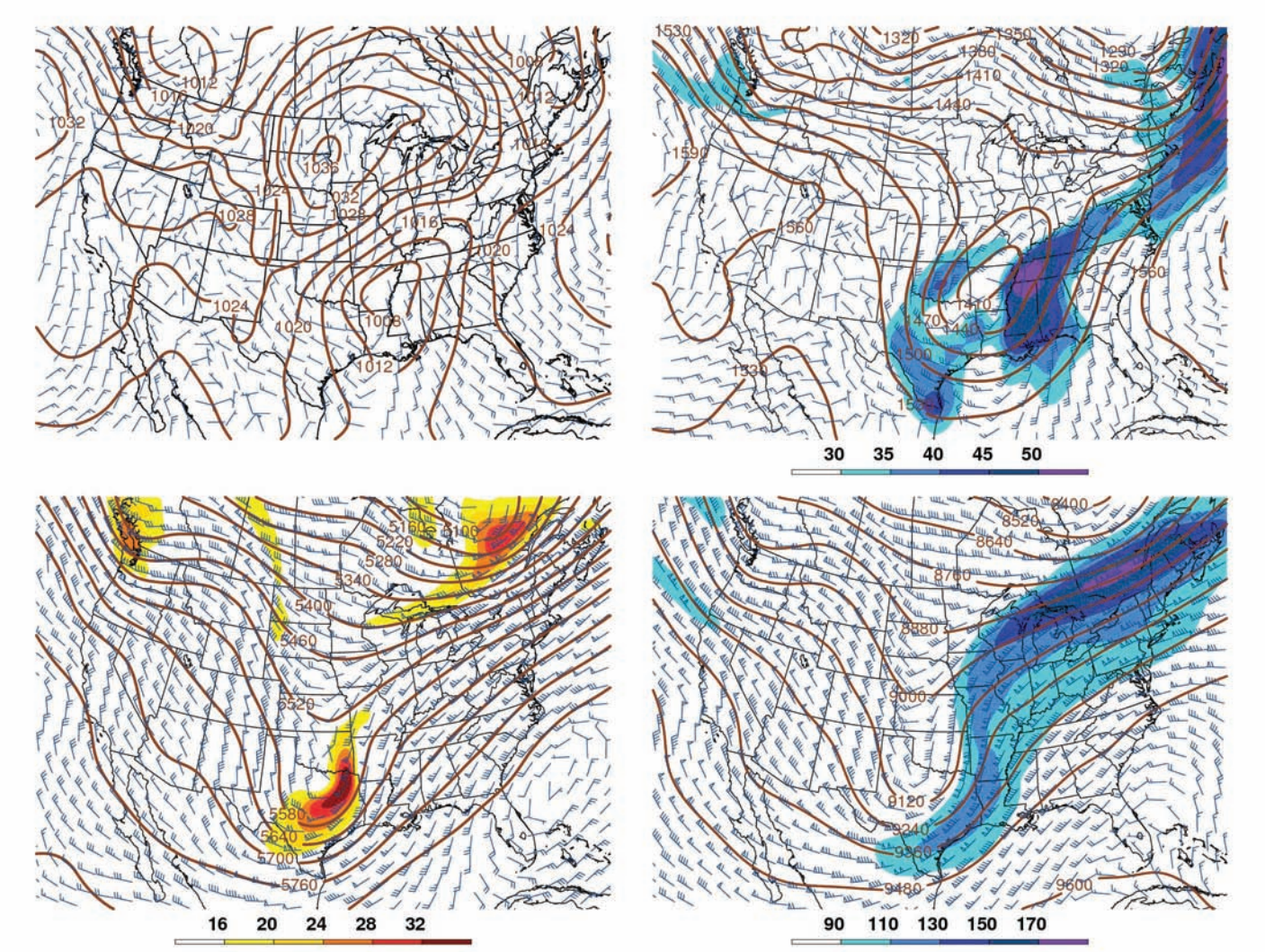

Fig. 13. Synoptic reanalysis from 0600 UTC 31 January 1982: (top left) mean sea-level pressure [solid brown, hPa] and 10-m wind [barbs, kts]; (top right) 850-hPa geopotential height [solid brown, m], isotachs [shaded, kts], and wind [barbs, kts]; (bottom left) 500-hPa geopotential height [solid brown, m], wind [barbs, kts], and absolute vorticity [shaded, 10^{-5} s^{-1}] ; (bottom right)300-hPa geopotential height [solid brown, m], isotachs [shaded, kts], and wind [barbs, kts].

The synoptic-scale flow evolution of the aforementioned case closely mirrored that of the composite mean. The tracks of both the surface and 850-hPa lows were nearly coincident, with the 30 January - 01 February 1982 case deepening more substantially. The 500-hPa shortwave troughs transitioned from positive to negative tilt with the 30 January - 01 February case exhibiting a more amplified trough. At 300 hPa, favorable jet-streak interaction was common to both the case study and composite mean. Stronger forcing for large-scale ascent was observed in the 30 January - 01 February 1982 case due to stronger Q-vector convergence and a better-defined upper-level cyclonic PV anomaly. Although the 30 January - 01 February case was an extremely heavy snowfall event for portions of the mid-Mississippi Valley, many of the significant synoptic-scale features and processes evolved analogously to the composite mean.

c. Mesoscale evolution

Strong mesoscale forcing separated the 30 January - 01 February 1982 case from a more typical heavy snow event in the mid-Mississippi Valley (i.e., compared to the composite values). The 850-hPa frontogenesis at 0600 UTC 31 January was oriented southwest-northeast from western Arkansas through southern Missouri into central Ohio (Fig. 17, top-left panel). The midlevel frontogenetical axis tilted northwestward with height as the 700-hPa

axis (Fig. 17, bottom-left panel) transversed from near Tulsa, Oklahoma to Indianapolis, Indiana. Similar to the composites (see Fig. 10, top-left and top-right panels), the northwest tilt with height is indicative of a direct thermal circulation over central and southern Missouri. Six hours later, the frontogenetical axis had translated to the northeast, paralleling the path of the midlevel low. Maximum values of 850-hPa frontogenesis between 0600 and 1200 UTC 31 January (Fig. 17, top-left and top-right panels) were approximately four times those found in the composite mean (see Fig. 10, top-left and top-right panels).

Cross-sections were analyzed for the 30 January - 01 February 1982 case at 0600 UTC (Fig. 18) and 1200 UTC 31 January (Fig. 19) respectively. Isentropes of θ_{es} revealed a convectively unstable environment to the southeast of the frontogenetical axis at 0600 UTC (Fig. 18, top panel). Some evidence of this reduced stability was observed above the layer of frontogenesis as the 320-K isentrope was approximately vertical (Fig. 18, top panel) and a wedge of negative EPV values extended to the northwest across western Kentucky and Tennessee (not shown). Convective instability in this case study was associated with several reports of thunder and lightning that accompanied the heavy snow across eastern Missouri.

Similar to the composite cross-sections, evidence of the cross-hair signature was also seen in the 30 January - 01 February 1982 case as the maximum UVM extended vertically into the DGZ at 0600 UTC 31 January (Fig. 18, bottom panel). However, the strength of the UVM was more pronounced with an area of supersaturation (RelHI ≥ 100%) within the DGZ for the 30 January - 01 February case compared to the composite mean. Furthermore, the RelHI and vertical motion fields were nearly perpendicular to the ground (Fig. 18, bottom panel), which also is suggestive of upright convection. Atmospheric stability

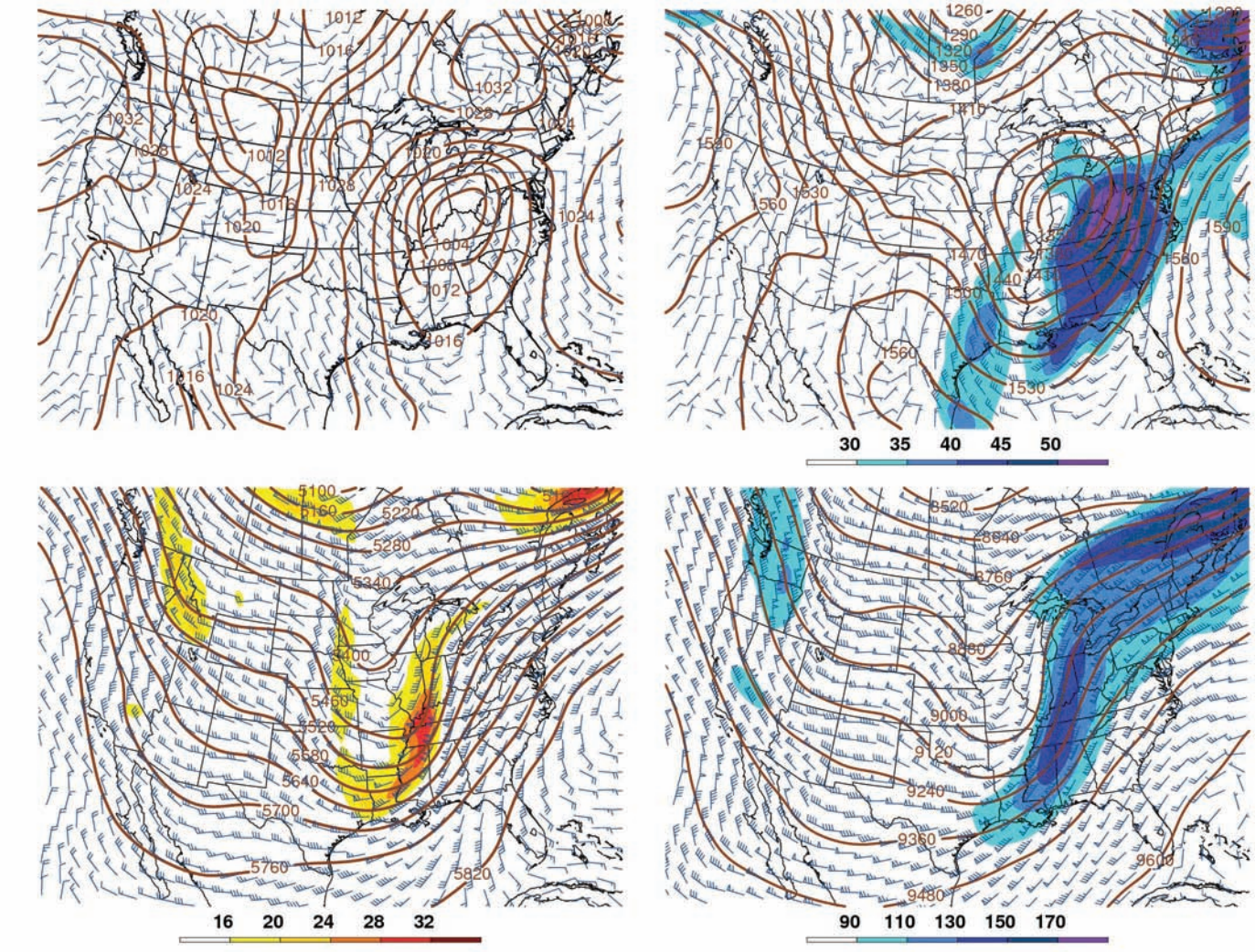

Fig. 14. As in Fig. 13, except for 1800 UTC 31 January 1982.

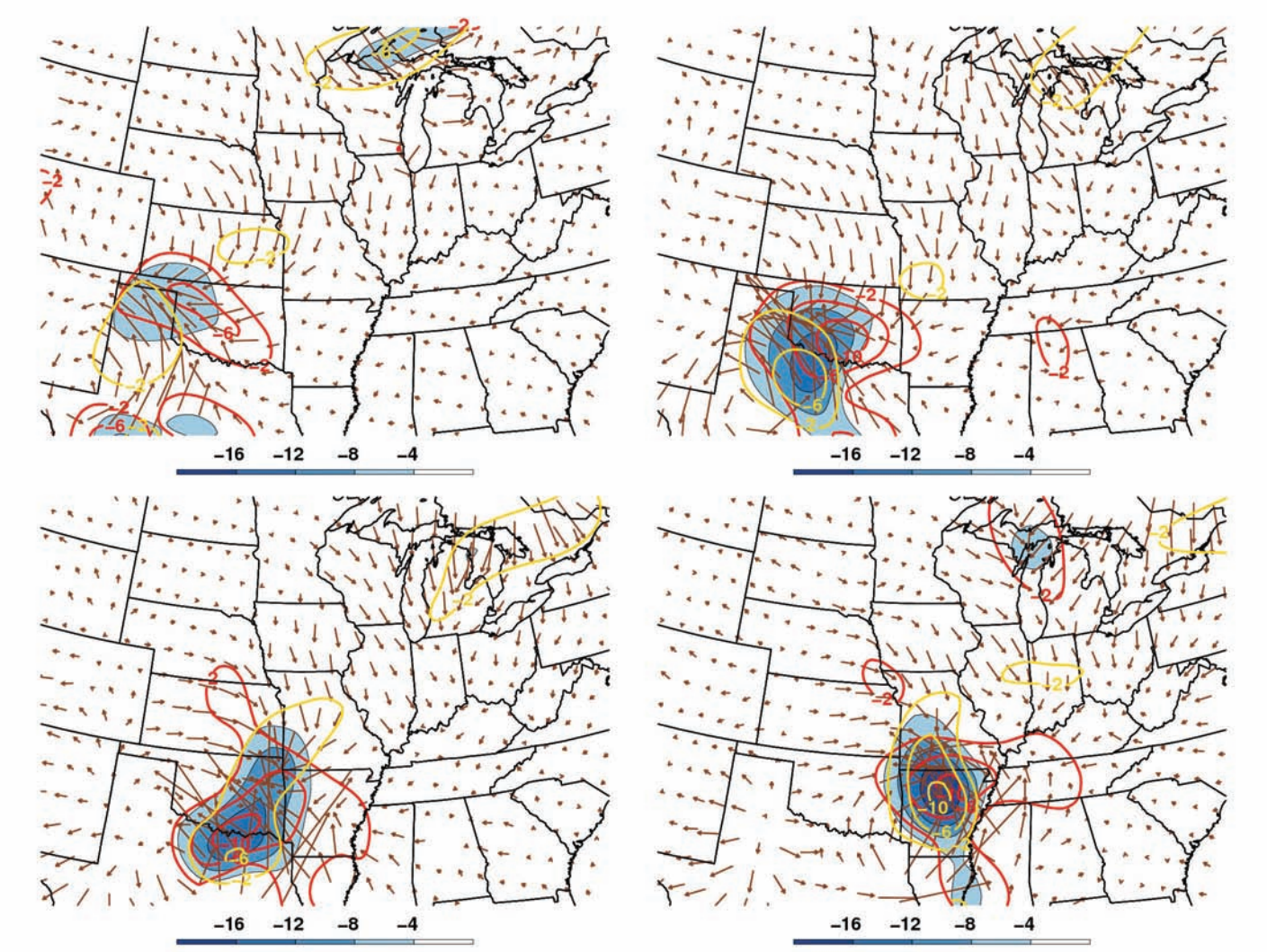

Fig. 15. Q vectors in the 400-hPa to 700-hPa layer [arrows, 10^{-10} K m^{-1} s^{-1}], convergence of total Q [shaded, 10^{-14} K m^{-2} s^{-1}], convergence of Qn [solid gold, 10^{-14} K m^{-2} s^{-1}], and convergence of Qs [solid red, 10^{-14} K m^{-2} s^{-1}]: (top left) 1800 UTC 30 January 1982, (top right) 0000 UTC 31 January 1982, (bottom left) 0600 UTC 31 January 1982, and (bottom right) 1200 UTC 31 January 1982.

increased by 1200 UTC as the RelHI and vertical motion fields became more tilted, suggesting more slantwise instability (Fig. 19, bottom panel) instead of upright convective instability. The UVM weakened by 1200 UTC 31 January and the maximum was now located below the DGZ (Fig. 19, bottom panel) in a temperature range more conducive to hollow columns as the predominant crystal shape instead of dendrites.

5. Case Variability

In addition to a single case comparison, it is also important to compare all the individual cases with the composited fields to provide a measure of the variability within the cases chosen for the compositing procedure. This assists in determining how representative the composite fields are of the typical conditions associated with heavy snowfall events within this region.

The linear spatial correlation coefficient between the 36 individual cases and the composite fields at the initial analysis time was computed to examine the robustness of the composite fields. The correlation is computed with the composite field shifted so that the 850-hPa low is collocated with the 850-hPa low of each case. The linear spatial correlation coefficient as used in Snedecor and Cochran (1967) is defined as

$$\mathrm{COR} = \frac{\frac{1}{N}\sum_{i=1}^{N}(X_i - \overline{X})(Y_i - \overline{Y})}{S_x S_y} \qquad (1)$$

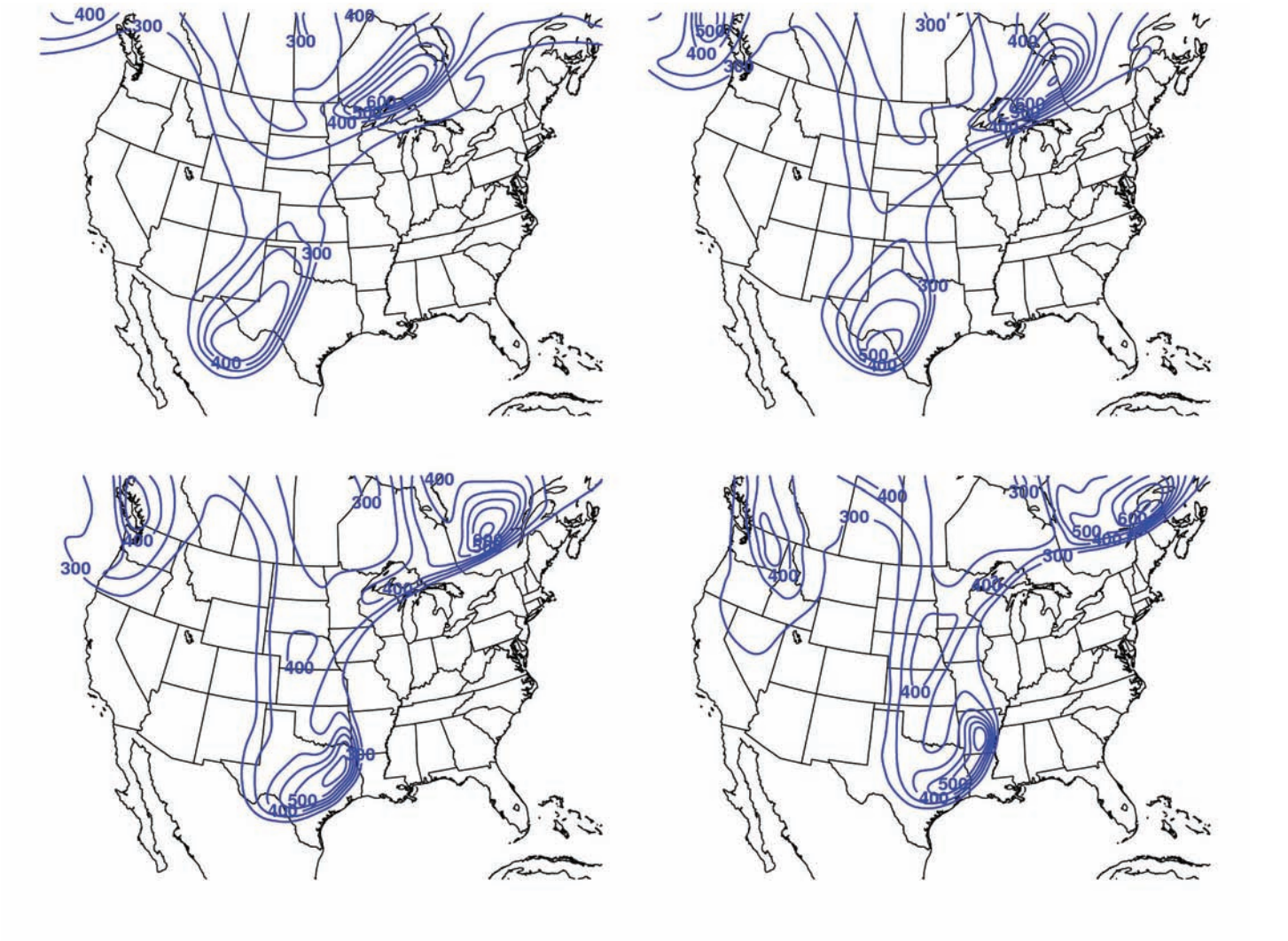

Fig. 16. Pressure [solid blue, hPa] on the 1.5 PVU surface for (top left) 1800 UTC 30 January 1982, (top right) 0000 UTC 31 January 1982, (bottom left) 0600 UTC 31 January 1982, and (bottom right) 1200 UTC 31 January 1982.

where N represents the total number of locations (i.e., grid points), X represents the field of an individual case, i represents all of the geographic locations (i.e., grid points), $\overline{X}$ is the spatial average of X, and S_x is the standard deviation of the individual case. The variable Y represents the same parameter as X, but for the composite field. The purpose of computing the correlation coefficient is to quantify the relative similarity of pattern between the individual cases and the composite.

Correlation coefficients for both the 300- and 500-hPa height fields were computed on a regional domain to capture features at the macro-β scale while all other fields were calculated on a subregional domain to capture features at the meso-α scale [as illustrated in Fig. 20, with scales defined by Orlanski (1975)]. High values of the correlation coefficient indicate that there is good agreement between the pattern of the composite field and that of the individual case. On the other hand, low or negative correlations indicate poor agreement between the pattern of the composite field and the individual case. This can occur for a variety of reasons including: (1) a shift (relative to the 850-hPa low center) in the individual case which departs from the composite pattern, (2) a unique pattern in the individual case not shown in the composite pattern, or (3) a reversal of the pattern from the composite field (Moore et al. 2003).

The distributions of correlations from several fields are displayed in box-and-whisker plots in Fig. 21. The 300- and 500-hPa height fields have high correlation coefficients with median values of 0.973 and 0.969 respectively. Additionally, there is little variability between the 90th and 10th percentiles for each of these

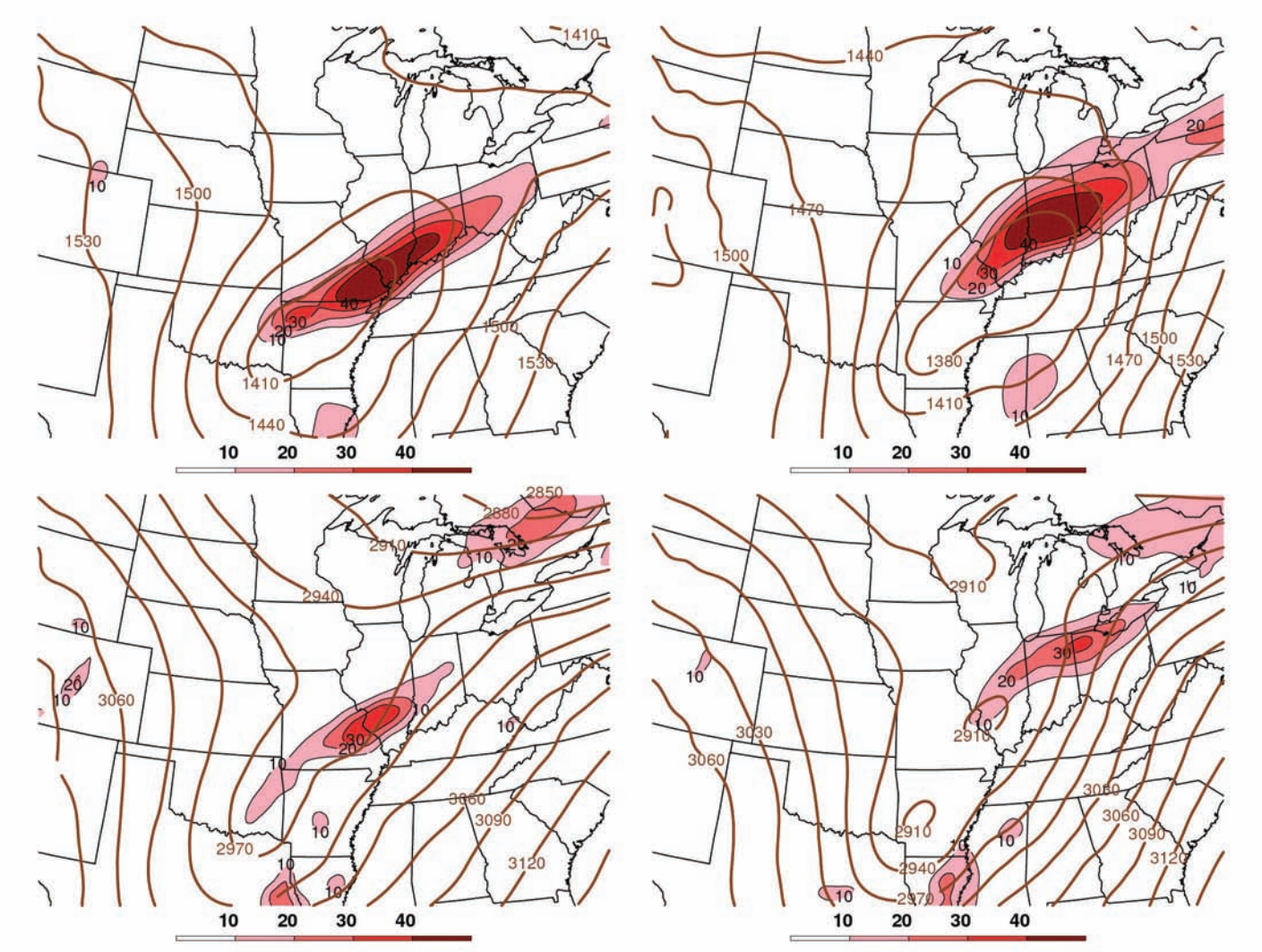

Fig. 17. 850-hPa geopotential height [solid brown, m] and frontogenesis [shaded, 10^{-1} K (100 km)$^{-1}$ (3 h)$^{-1}$] from reanalysis: (top left) valid at 0600 UTC 31 January 1982 and (top right) for 1200 UTC 31 January; 700-hPa geopotential height [solid brown, m] and frontogenesis [shaded, 10^{-1} K (100 km)$^{-1}$ (3 h)$^{-1}$]: (bottom left) valid at 0600 UTC 31 January and (bottom right) for 1200 UTC 31 January.

fields, indicating that the patterns seen at 300 and 500 hPa are not only well-correlated with the composite mean; but are also highly consistent. To illustrate this measure of agreement, the 300- and 500-hPa height correlations from the 30 January - 01 February 1982 case (cf. Fig. 5 and Fig. 13) are 0.989 and 0.987. Mean sea-level pressure, precipitable water, and height, temperature, isotach, and mixing ratio fields at 850 hPa also have high correlation coefficients with median values ranging from 0.725 to 0.943. The slight increase in variability among the cases results in lower correlations and a larger spread. Fields that had low correlation coefficients included 850- and 700-hPa frontogenesis and 400-700-hPa layer total Q-vector convergence with median values of 0.352, 0.339, and 0.136 respectively. Furthermore, the distance between the 90th and 10th percentiles for these fields is much greater than those previously examined. The localized nature of key features (e.g., the low-level frontogenesis axis to the northwest of the surface cyclone) can be partially masked by other variability within the subregional domain which reduces the overall correlation. For example, the correlation in frontogenesis can be reduced by variability in frontogenesis along the surface cold front. The member with the second highest overall correlation (sum of the individual correlations) was the 30 January - 01 February 1982 event, which explains why this particular case was one of the most representative of the composite mean and warranted detailed examination.

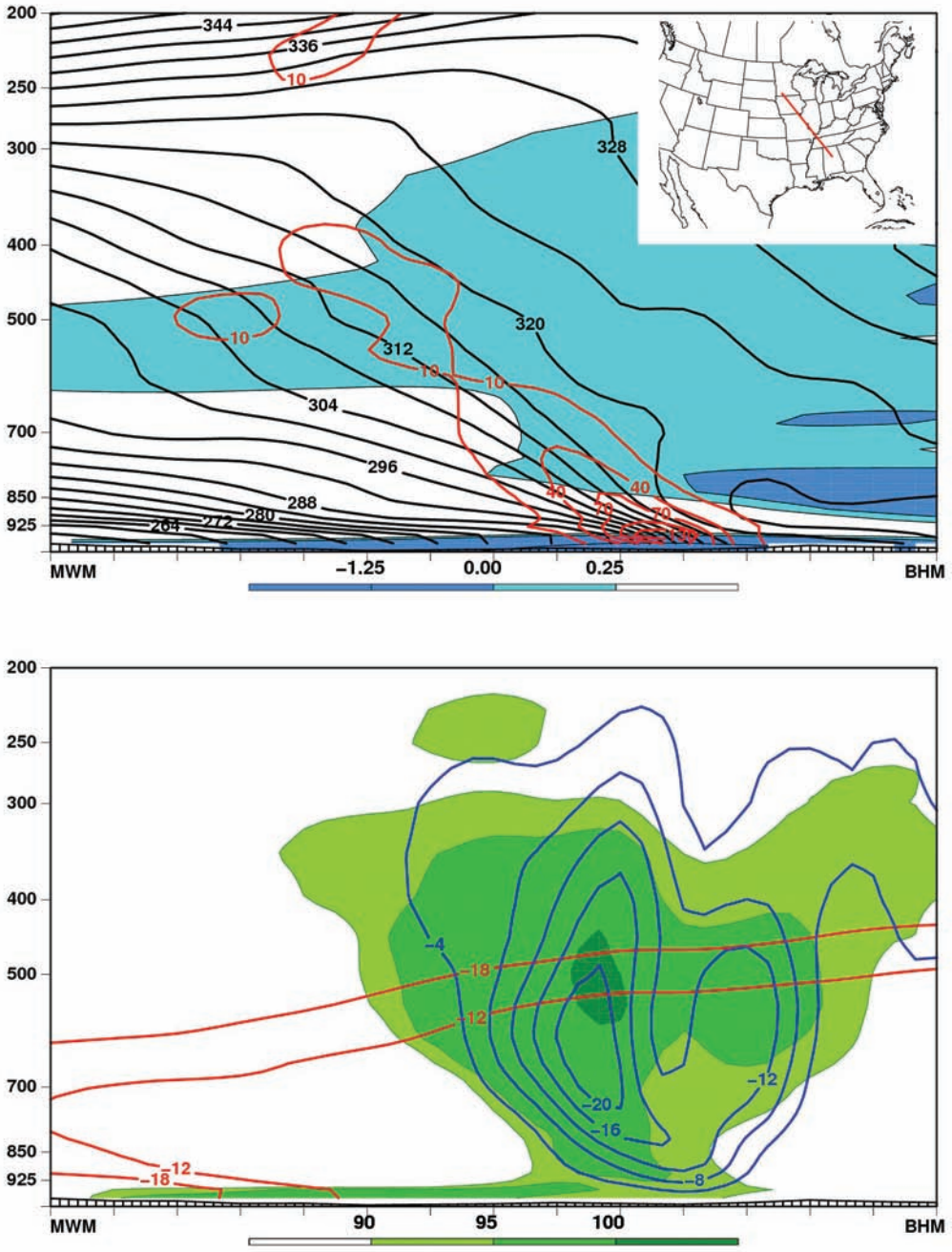

Fig. 18. (top panel) Cross-section showing equivalent potential vorticity [shaded, 10^{-6} K kg^{-1} m^2 s^{-1}], saturation equivalent potential temperature [solid black, K], and frontogenesis [solid red, 10^{-1} K (100 km)$^{-1}$ (3 h)$^{-1}$] from 0600 UTC 31 January 1982; and (bottom panel) cross-section showing omega [solid blue, μb s^{-1}], relative humidity with respect to ice beginning at 90% [shaded], and the dendritic growth zone from -12^{0}C to -18^{0}C [solid red, ^{0}C] from 0600 UTC 31 January (bottom). Inset figure depicts the orientation of the cross-section.

Outliers were found in both the 850-hPa height and mean sea-level pressure fields. The lowest correlation value was 0.587 for 850-hPa geopotential height and 0.150 for mean sea-level pressure, which were both well below the 10th percentile for their respective fields. An overlay of the composite mean field and the associated case outlier can be seen in Fig. 20. The 850-hPa low at 1800 UTC 03 March 1999 was displaced to the south of the composite 850-hPa low with a west-east orientation to the trough axis (Fig. 20, top panel) instead of southwest-northeast as seen in the composite field. This west-to-east orientation resulted in a lower correlation value most likely due to

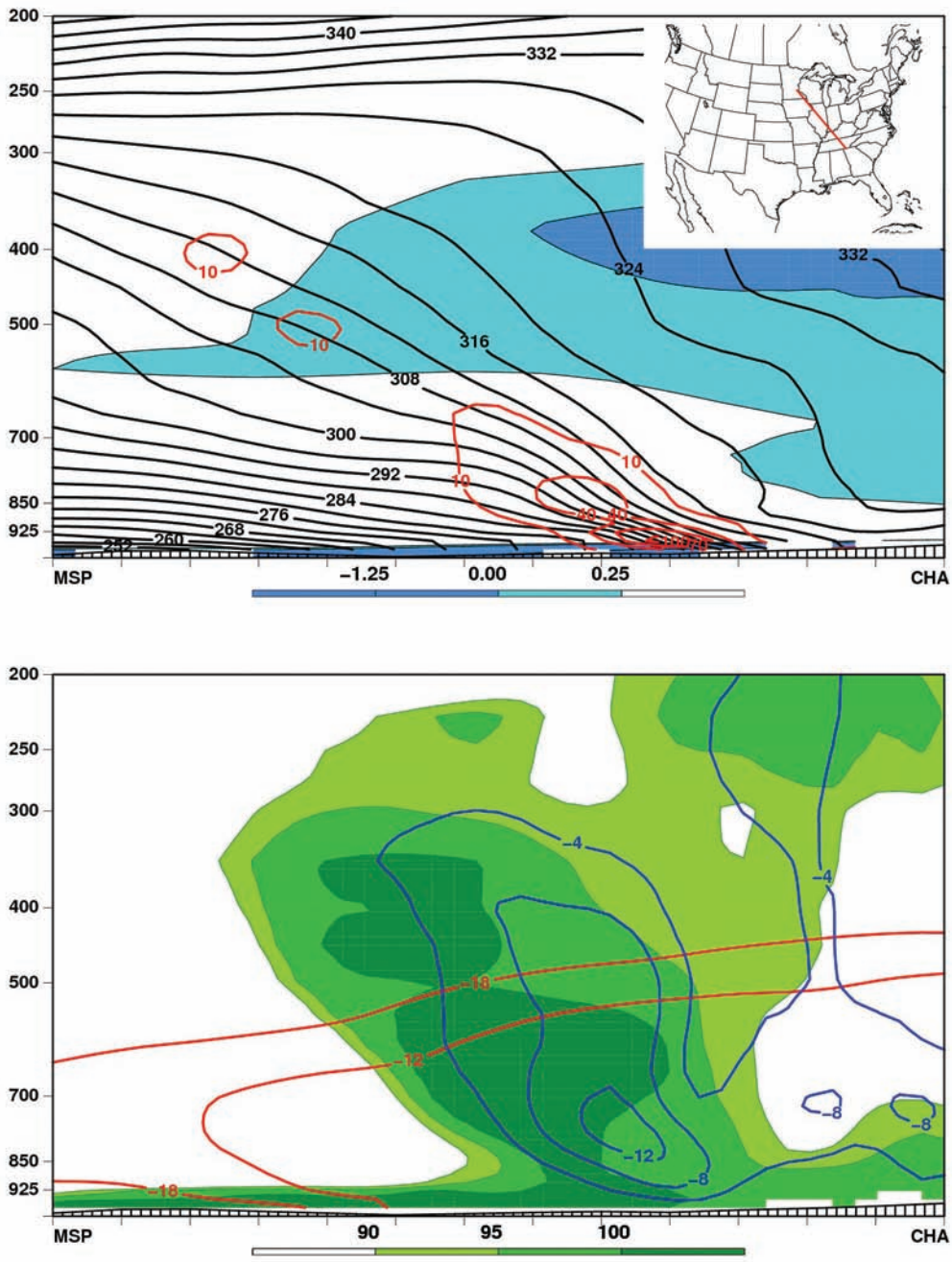

Fig. 19. As in Fig. 18, except for 1200 UTC 31 January 1982.

differences in the height gradient toward the western and eastern edges of the subregional domain. The surface low at 1800 UTC 09 January 1987 (Fig. 20, bottom panel) was elongated, with a 1012-hPa closed contour centered to the north and west of the composite surface cyclone. In this particular case, a rapidly occluding system developed a unique surface pattern, which resulted in a lower correlation value. In spite of these lower correlations, the overall structure of the surface and 850-hPa systems for these cases still retain many of the features found in the composite.

6. Conclusions

The composite analysis of heavy snow events depicted the environmental conditions and their evolution, which can aid forecasters in anticipating heavy snowfall associated with a common cyclone track in the mid-

Mississippi Valley. The four-dimensional midlatitude cyclone tilted westward with height while strengthening throughout the duration of the compositing period. This strengthening is associated with persistent large-scale ascent through jet-streak interaction and differential positive vorticity advection. In addition, the composite cyclone took a favorable track for heavy snowfall as the surface and 850-hPa low centers passed to the south and east of the region. As the system entered the area of interest, an increase in mesoscale forcing was observed to develop over the study area due to strengthening low-level frontogenesis and reduced stability coincident with an intensifying low-level jet. Further evidence of UVM was found through Q-vector diagnostics on both the synoptic scale (i.e., Q_s) and mesoscale (i.e., Q_n).

Air flow associated with the TROWAL airstream encountered a region of enhanced ascent from mesoscale processes to the northwest of the cyclone. The UVM occurred within a temperature range supportive of dendritic ice crystal growth, which increased the efficiency (i.e., increased the snow-to-liquid ratio) of the snowfall. While the focus of this paper was on the SGF and LSX NWS CWAs, the majority of these systems produced heavy snowfall downstream from the region of interest. Consequently, these results could also be used in anticipating heavy snowfall in regions to the north and east.

The composite results largely confirm previous research (e.g., Mote et al. 1997; Martin 1998; Novak et al. 2010) regarding the synoptic and mesoscale conditions favorable for heavy snowfall. It is important to note that these results were a compilation of 36 heavy snow cases (Table 1) in the SGF and LSX CWAs. The attendant processes and their evolution seen in the composite mean fields were persistent enough to manifest themselves in the composites. However, by examining only heavy snow events, the composite fields' ability to predict heavy snow has not been considered. A composite study of null events (presence of similar patterns that do not yield heavy snow) is an area of future research.

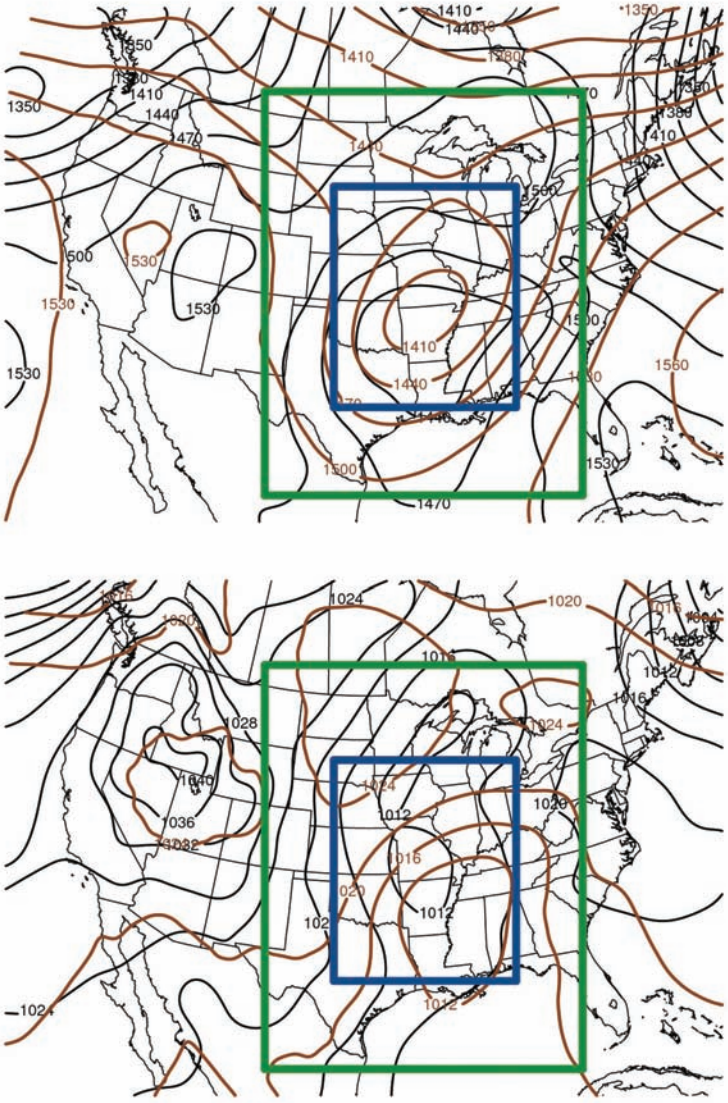

Fig. 20. (top panel) Composite 850-hPa geopotential height [thick brown, m] at t = 0 h and 850-hPa geopotential height [thin black, m] from synoptic reanalysis at 1800 UTC 03 March 1999, and (bottom panel) composite mean sea-level pressure [thick brown, hPa] at t = 0 h and mean sea-level pressure [thin black, hPa] from synoptic reanalysis at 1800 UTC 09 January 1987. Green outline [solid] is the regional domain and the blue outline [solid] is the subregional domain for the statistical correlations.

Authors

Jayson P. Gosselin is currently a meteorological intern at the National Weather Service Forecast Office in St. Louis, Missouri. He recently received his Master of Science degree in Meteorology from Saint Louis University in 2010, researching central and northeastern United States heavy snow events. He also graduated from Saint Louis University with a Bachelor of Science degree in May 2004. Primary research interests are high impact winter weather events, with a focus on heavy snow.

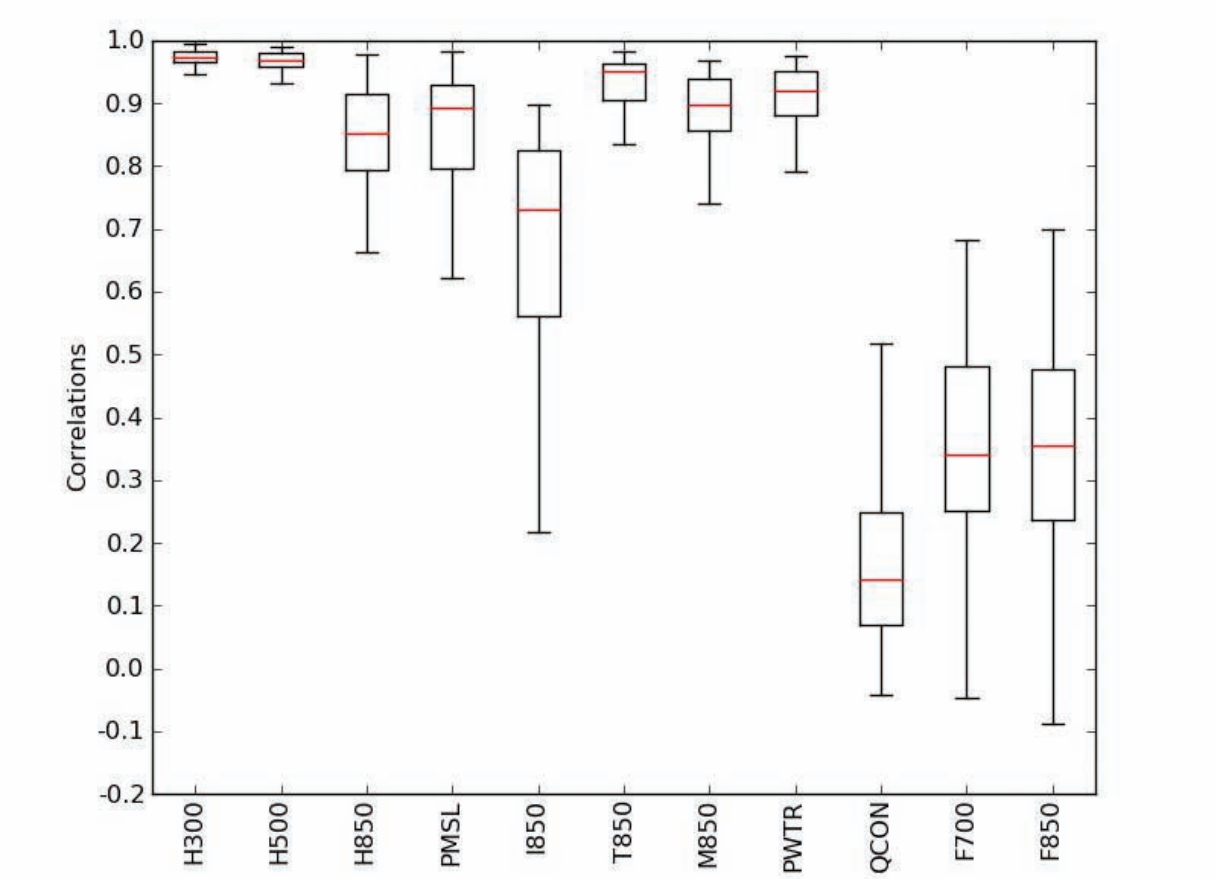

Fig. 21. Box-and-whisker plots displaying the range in correlations between the composite fields and the individual cases. The horizontal line (red) within each box represents the 50th percentile, the top (bottom) line of the box is the 75th (25th) percentile, and the top (bottom) line outside the box represents the 90th (10th) percentile. Composite fields examined were: H300, 300-hPa geopotential height; H500, 500-hPa geopotential height; H850, 850-hPa geopotential height; PMSL, mean sea-level pressure; I850, 850-hPa isotach; T850, 850-hPa temperature; M850, mixing ratio at 850 hPa; PWTR, precipitable water; QCON, 400-700-hPa layer total Q-vector convergence; F700, 700-hPa frontogenesis; F850, 850-hPa frontogenesis. H300 and H500 correlations were taken with respect to the regional domain (green outline) while all other variable correlations were taken with respect to the subregional domain (blue outline).

Chad M. Gravelle is currently a Ph.D. candidate at Saint Louis University in St. Louis, MO under the supervision of Dr. Charles E. Graves. He received his Master of Science degree in Meteorology from Saint Louis University in 2007 and his Bachelor of Science degree from The College at Brockport, State University of New York in 2005. Chad's research is operationally focused with an emphasis on winter weather and his dissertation will verify and examine the robustness of the northeastern United States heavy snow conceptual model.

Charles E. Graves is currently an Associate Professor in the Department of Earth and Atmospheric Sciences at Saint Louis University. He received his Ph.D. in Physics from Iowa State University in 1988. After a post-doctoral position at Texas A&M, he became an Assistant Professor at Saint Louis University in 1992. Dr. Graves' research interests are in operational meteorology with an emphasis on heavy precipitation.

John P. Gagan is currently a Senior Forecaster at the National Weather Service Forecast Office in Springfield, Missouri. He received his Master of Science degree in Meteorology from Saint Louis University in 2001, with research focused on heavy rainfall and the role of system propagation. John began his weather career as a Medium-range Forecaster and Weather Derivative Trader for Aquila Energy, based in Kansas City, MO. He began his NWS career as a General Forecaster in Jackson, MS from late 2002 through early 2006. John's research interests have been focused on the improvement of weather forecasts, with an emphasis in the early detection and risk assessment of hazardous, high impact weather events.

Fred Glass is a Senior Meteorologist at the National Weather Service Forecast Office in St. Louis, Missouri, a position he has held since summer 1993. Previously he served as a Journeyman Forecaster at the NWS St. Louis Office, as well as a Developmental Forecaster and Meteorological Intern in the Forecast Branch/ Meteorological Operations Division of the National Meteorological Center. He earned a B.S. degree in Meteorology from the University of Oklahoma (OU) in 1986, and worked as a Graduate Research Assistant and Computer Programmer in 1986-87 for the Cooperative Institute for Mesoscale Meteorological Systems at the National Severe Storms Lab while pursuing graduate studies at OU. He is the author or co-author of numerous conference papers on the topics of heavy rainfall, flash flooding, and severe convective storms, and has also conducted a number of related conference workshops.

References

Adams, R. M., L. L. Houston, and R. F.Weiher, cited 2004: The value of snow and snow information services. [Available online at www.economics.noaa.gov/bibliography/econ-value-snow-final-report.doc].

Barnes, S. L., 1973: Mesoscale objective analysis using weighted time-series observations. NOAA Tech. Memo. ERL NSSL-62, 60 pp. [NTIS COM-73-10781].

Baxter, M. A., C. E. Graves, and J. T. Moore, 2005: A climatology of snow-to-liquid ratio for the contiguous United States. *Wea. Forecasting*, 20, 729-744.

Brandes, E. A. and J. Spar, 1971: A search for necessary conditions for heavy snow on the East Coast. *J. Appl. Meteor.*, 11, 397-409.

Brennan, M. J., G. M. Lackmann, and K. M. Mahoney, 2007: Potential vorticity (PV) thinking in operations: The utility of nonconversation. *Wea. Forecasting*, 23, 168-182.

Browne, R. F. and R. J. Younkin, 1970: Some relationships between 850 millibar lows and heavy snow occurrences over the central and eastern United States. *Mon. Wea. Rev.*, 98, 399-401.

Changnon, S. A., 1969: Climatology of severe winter storms in Illinois. Bulletin 53, Illinois State Water Survey, Champaign, IL, 52 pp.

_____and D. Changnon, 1978: Record winter storms in Illinois, 1977-1978. Report of Investigation 88, Illinois State Water Survey, Champaign, IL, 23 pp.

Acknowledgments

The authors would like to thank Scott Rochette (The College at Brockport, State University of New York) for taking the time to review this manuscript and William Davis, Meteorologist-In-Charge (MIC), NOAA/NWS Springfield, Missouri, Wes Browning, MIC, NOAA/NWS St. Louis, Missouri, Ron Przybylinski Science and Operations Officer (SOO), NOAA/NWS St. Louis, Missouri, and Dave Gaede, SOO, NOAA/NWS Springfield, Missouri for supporting this project.

_____, _____, and T. R. Karl, 2006: Temporal and spatial characteristics of snowstorms in the contiguous United States. *J. Appl. Meteor. Climatol*., 45, 1141-1155.

desJardins, M. L., K. F. Brill, and S. S. Schotz, 1991: Use of GEMPAK on UNIX work-stations. *Proc., 7th Intl. Conf. on Interactive Information and Processing Systems for Meteorology, Oceanography, and Hydrology*. New Orleans, LA. Amer. Meteor. Soc., 449-453.

Doesken, N. and A. Judson, 1996: *The Snow Booklet: A Guide to the Science, Climatology, and Measurement of Snow in the United States*. Colorado State University Dept. of Atmospheric Science, 84 pp.

Emanuel, K. A., 1985: Frontal circulations in the presence of small moist symmetric stability. *J. Atmos. Sci*., 42, 1062-1071.

Fawcett, E. B. and H. K. Saylor, 1965: A study of the distribution of weather accompanying Colorado cyclongenesis. *Mon. Wea. Rev*., 93, 359-367.

Goree, P. A. and R. J. Younkin, 1966: Synoptic climatology of heavy snowfall over the central and eastern United States. *Mon. Wea. Rev*., 94, 663-668.

Hoskins, B. J., I. Draghici, and H. C. Davies, 1978: A new look at the ω-equation. *Quart. J. Roy. Meteor. Soc*., 104, 31-38.

Keyser, B. D., B. D. Schmidt, and D. G. Duffy, 1992: Quasigeostrophic vertical motions diagnosed from along- and cross-isentrope components of the Q vector. *Mon. Wea. Rev*., 120, 731-741.

Kocin, P. J. and L. W. Uccellini, 2004: Synoptic descriptions of major snowstorms: Upper-level features. *Northeast Snowstorms*. *Vol. 1, Meteor.Monogr*., No. 54, Amer. Meteor. Soc., 79-142.

Martin, J. E., 1998: The structure and evolution of a continental winter cyclone. Part I: Frontal structure and the occlusion process. *Mon. Wea. Rev*., 126, 303--328.

Mesinger, F. and Coauthors, 2006: North American Regional Reanalysis. *Bull. Amer. Meteor. Soc*., 87, 343--360.

Moore, J. T. and P. D. Blakely, 1988: The role of frontogenetical forcing and conditional symmetric instability in the Midwest snowstorm of 30-31 January 1982. *Mon. Wea. Rev*., 116, 2155-2171.

_____, F. H. Glass, C. E. Graves, S. M. Rochette, and M. Singer, 2003: The environment of warm-season elevated thunderstorms associated with heavy rainfall over the central United States. *Wea. Forecasting*, 18, 861-878.

Mote, T. L., D. W. Gamble, S. J. Underwood, and M. L. Bentley, 1997: Synoptic-scale features common to heavy snowstorms in the Southeast United States. *Wea. Forecasting*, 12, 5-23.

Novak, D. R., L. F. Bosart, D. Keyser, and J. S. Waldstreicher, 2004: An observational study of cold season-banded precipitation in Northeast U.S. cyclones. *Wea. Forecasting*, 19, 993-1010.

_____, B. A. Colle, and A. R. Aiyyer, 2010: Evolution of mesoscale precipitation band environments within the comma head of Northeast U.S. cyclones. *Mon. Wea. Rev*., 138, 2354-2374 .

Orlanski, I., 1975: A rational subdivision of scales for atmospheric processes. *Bull. Amer. Meteor. Soc*., 56, 527-530.

Posselt, D. J. and J. E. Martin, 2004: The effect of latent heat release on the evolution of a warm occluded thermal structure. *Mon. Wea. Rev*., 132, 578-599.

Pruppacher, H. R. and J. D. Klett, 1997: *Microphysics of Clouds and Precipitation*. Kluwer Academic, 954 pp.

Schmit, L. and T. Hultquist, 2009: A synoptic climatology of winter storms in the Twin Cities area. Preprints, *23rd Conf. on Weather Analysis and Forecasting*, Omaha, NE, Amer. Meteor. Soc., CD-ROM, JP3.8.

Snedecor, G. W. and W. G. Cochran, 1967: *Statistical Methods*. 6th ed. The Iowa State University Press, 593 pp.

Waldstreicher, J. S., cited 2001: The importance of snow microphysics for large snowfalls. [Available online at http://www.erh.noaa.gov/er/hq/ssd/snowmicro/sld001.html]